Engineering Geology xxx (2008) xxx–xxx

Contents lists available at ScienceDirect

Engineering Geology

journal homepage: www.elsevier.com/locate/enggeo

Spatial data for landslide susceptibility, hazard, and vulnerability assessment: An overview

Cees J. van Westen *, Enrique Castellanos, Sekhar L. Kuriakose

International Institute for Geo-Information Science and Earth Observation, ITC, P.O. Box 6, 7500 AA Enschede, The Netherlands

ARTICLE INFO

Article history:
Accepted 4 March 2008
Available online xxxx

Keywords:
Spatial data
Landslides
Landslide inventory mapping
Environmental factors
Triggering factors
Elements at risk

ABSTRACT

The aim of this paper is to discuss a number of issues related to the use of spatial information for landslide susceptibility, hazard, and vulnerability assessment. The paper centers around the types of spatial data needed for each of these components, and the methods for obtaining them. A number of concepts are illustrated using an extensive spatial data set for the city of Tegucigalpa in Honduras. The paper intends to supplement the information given in the "Guidelines for Landslide Susceptibility, Hazard and Risk Zoning for Land Use Planning" by the Joint ISSMGE, ISRM and IAEG Technical Committee on Landslides and Engineered Slopes (JTC-1). The last few decades have shown a very fast development in the application of digital tools such as Geographic Information Systems, Digital Image Processing, Digital Photogrammetry and Global Positioning Systems. Landslide inventory databases are becoming available to more countries and several are now also available through the internet. A comprehensive landslide inventory is a must in order to be able to quantify both landslide hazard and risk. With respect to the environmental factors used in landslide hazard assessment, there is a tendency to utilize those data layers that are easily obtainable from Digital Elevation Models and satellite imagery, whereas less emphasis is on those data layers that require detailed field investigations. A review is given of the trends in collecting spatial information on environmental factors with a focus on Digital Elevation Models, geology and soils, geomorphology, land use and elements at risk.

1. Introduction

The first extensive papers on the use of spatial information in a digital context for landslide susceptibility mapping date back to the late seventies and early eighties of the last century. Among the pioneers in this field were Brabb et al. (1978) in California and Carrara et al. (1977) in Italy. Nowadays, practically all research on landslide susceptibility and hazard mapping makes use of digital tools for handling spatial data such as GIS, GPS and Remote Sensing. These tools also have defined, to a large extent, the type of analysis that can be carried out. It can be stated that GIS has determined, to a certain degree, the current state of the art in landslide hazard and risk assessment. Fig. 1, based on Van Westen et al. (2005) gives a schematic overview of the various components of landslide risk assessment. This paper intends to supplement the information given in the "Guidelines for Landslide Susceptibility, Hazard and Risk Zoning for Land Use Planning" by the Joint ISSMGE, ISRM and IAEG Technical Committee on Landslides and Engineered Slopes (JTC-1, 2008—this volume). A number of concepts are illustrated using a spatial data set for the city of Tegucigalpa, the capital of Honduras. Tegucigalpa was severely hit by both flooding and landslides, during the passing of hurricane Mitch in 1998, and over 1000 people were killed by landslides in the city, of which the landslides named El Berrinche and El Reparto were the largest ones (Harp et al., 2002a; Mastin, 2002).

2. Spatial data types

Table 1 gives a schematic overview of the main data layers required for landslide susceptibility, hazard and risk assessment (indicated in the upper row of Fig. 1). These can be subdivided into four groups: landslide inventory data, environmental factors, triggering factors, and elements at risk (Van Westen et al., 2005). Of these, the landslide inventory is by far the most important, as it should give insight into the location of landslide phenomena, the types, failure mechanisms, causal factors, frequency of occurrence, volumes and the damage that has been caused. Landslide inventory databases should display information on landslide activity, and therefore require multi-temporal landslide information over larger regions. For detailed mapping scales, activity analysis is often restricted to a single landslide and becomes more landslide monitoring. The environmental factors are a collection of data layers that are expected to have an effect on the occurrence of landslides, and can be utilized as causal factors in the prediction of future landslides. The list of environmental factors indicated in Table 1 is not exhaustive, and it is important to make a selection of the specific factors that are related to

* Corresponding author. Tel.: +31 53 4874263; fax: +31 53 4874336.
E-mail address: westen@itc.nl (C.J. van Westen).

0013-7952/$ – see front matter © 2008 Elsevier B.V. All rights reserved.
doi:10.1016/j.enggeo.2008.03.010

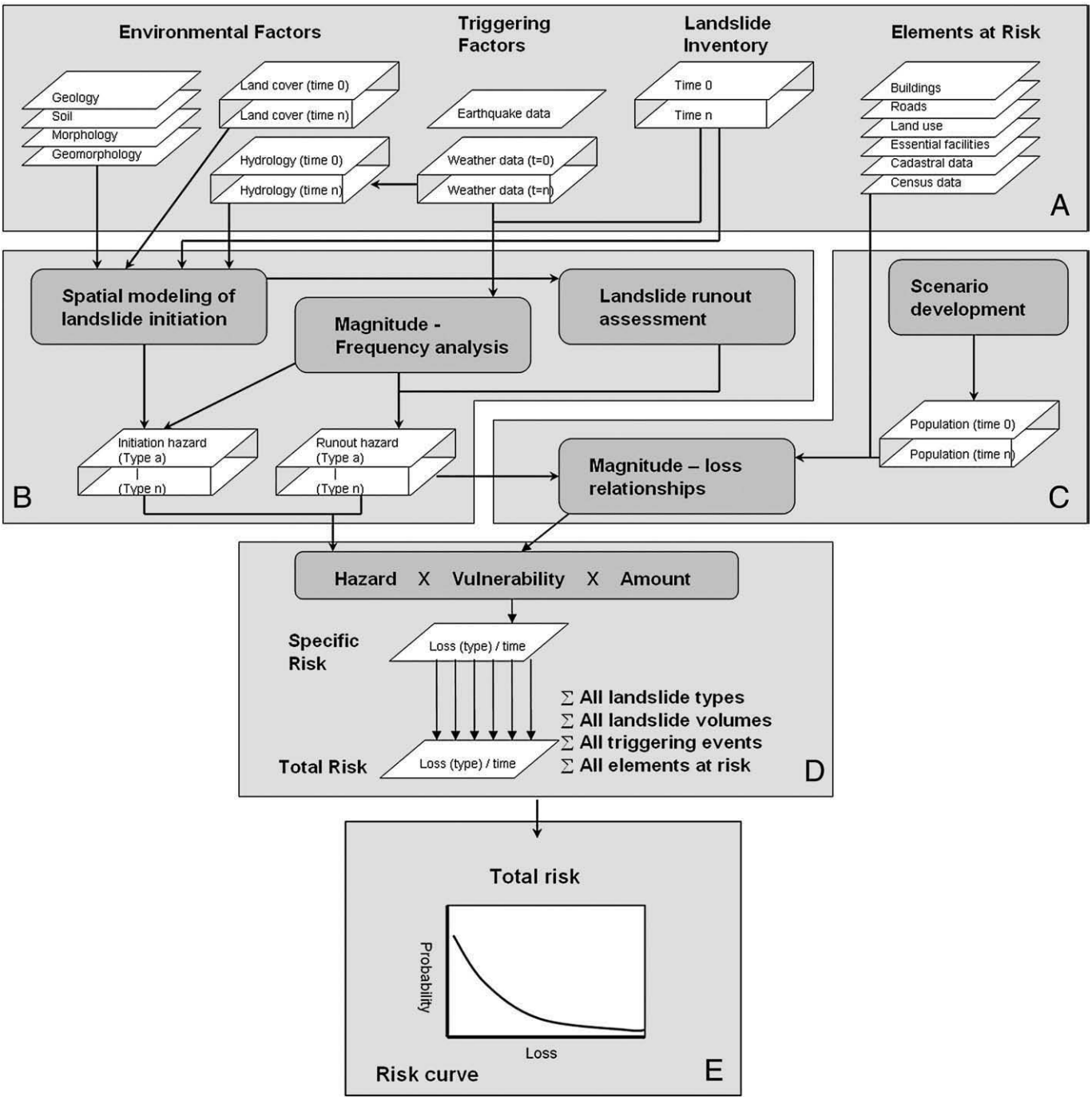

Fig. 1. Schematic representation of the landslide risk assessment procedure. A: Basic data sets required, both of static, as well as dynamic (indicated with "time…") nature, B: Susceptibility and hazard modeling component, C: Vulnerability assessment component, D: Risk assessment component, E: Total risk calculation in the form of a risk curve. See text for further explanation.

the landslide types and failure mechanisms in each particular environment (Cruden and Varnes, 1996). However, they do give an idea of the types of data included, related to morphometry, geology, soil types, hydrology, geomorphology and land use. It is not possible to give a prescribed uniform list of causal factors. The selection of causal factors differs, depending on the scale of analysis, the characteristics of the study area, the landslide type, and the failure mechanisms (Glade and Crozier, 2005). Table 1 intends to provide a summary of this discussion. The basic data can be subdivided into those that are more or less static, and those that are dynamic and need to be updated regularly (See Table 1). Examples of static data sets are related to geology, soil types, geomorphology and morphography. The time frame for the updating of dynamic data may range from hours to days, for example for meteorological data and its effect on slope hydrology, to months and years for land use and population data (see Table 1). Landslide information needs to be updated continuously, and land use and elements at risk data need to have an update frequency which may range from 1 to 10 years, depending on the dynamics of land use change in an area. Especially the land use information should be evaluated with care, as this is both an environmental factor, which determines the occurrence of new landslides, as well as an element at risk, which may be affected by landslides.

Please cite this article as: van Westen, C.J., et al., Spatial data for landslide susceptibility, hazard, and vulnerability assessment: An overview, Engineering Geology (2008), doi:10.1016/j.enggeo.2008.03.010

Table 1
Schematic representation of basic data sets for landslide susceptibility, hazard and risk assessment

Data		Update frequency (years)	RS	Scale			Hazard models				Risk methods	
Main Type	Data layer	10..... 1. ... 0.002 (day)	Remote Sensing useful?	Small	Medium	Large	Detailed	Heuristic	Statistical	Deterministic	Probabilistic	(Semi) Quantitative	Qualitative
Landslide Inventory	Landslide inventory		H	C	H	H	H	C	H	H	H	Requires results of probabilistic hazard analysis	Requires results of heuristic, statistical or deterministic hazard analysis
	Landslide activity		H	M	C	C	C	H	C	C	C		
	Landslide monitoring		M	M	M	M	C	-	-	H	H		
Environmental factors	DEM		H	H	C	C	C	H	C	C	C		
	Slope angle/aspects etc		H	L	H	H	H	H	H	H	H		
	Internal relief		H	H	M	L	L	H	L	-	-		
	Flow accumulation		H	L	M	H	H	L	M	H	H		
	Lithology		M	H	H	H	H	H	H	H	H		
	Structure		M	H	H	H	H	H	H	H	H		
	Faults		M	H	H	H	H	H	H	-	-		
	Soil types		M	M	H	C	C	H	H	C	H		
	Soil depth		-	-	L	C	C	-	-	C	H		
	Slope hydrology		-	-	-	C	C	-	-	C	H		
	Main geomorphology units		H	C	H	M	L	C	M	L	L		
	Detailed geomorph. units		H	H	H	H	L	H	H	M	L		
	Land use types		H	H	H	H	H	H	H	H	H		
	Land use changes		H	M	H	H	C	H	H	H	C		
Triggering factors	Rainfall		L	M	M	C	C	H	H	C	C		
	Temp / evapotranspiration		M	-	-	M	H	-	-	H	L		
	Earthquake catalogs		-	M	M	H	C	-	-	-	C		
	Ground acceleration		L	L	M	H	H	H	H	H	L		
Elements at risk	Buildings		H	L	M	C	C	-	-	-	-	C	C
	Transportation networks		H	M	M	M	H	M	M	M	M	H	H
	Lifelines		-	-	L	L	M	-	-	-	-	L	L
	Essential facilities		L	L	M	H	H	-	-	-	-	H	H
	Population data		L	H	H	C	C	-	-	-	-	C	C
	Agriculture data		H	L	M	H	M	-	-	-	-	L	M
	Economic data		-	L	M	H	H	-	-	-	-	L	M
	Ecological data		H	L	L	L	L	-	-	-	-	L	M

Left: indication of the main types of data, Middle: indication of the ideal update frequency, RS: column indicating the usefulness of Remote Sensing for the acquisition of the data, Scale: indication of the importance of the data layer at small, medium, large and detailed scales, related with the feasibility of obtaining the data at that particular scale, Hazard models: indication of the importance of the data set for heuristic models, statistical models, deterministic models, and probabilistic models, Risk models: indication of the importance of the data layer for qualitative and quantitative vulnerability and risk analysis. (C=Critical data set, H=highly important, M=moderately important, and L=Less important, –=Not relevant).

Table 1 also gives an indication of the extent to which remote sensing data can be utilized to generate the various data layers (based on Soeters and Van Westen, 1996, and Metternicht et al., 2005). For a number of data layers the main emphasis in data acquisition is on field mapping, field measurements or laboratory analysis, and remote sensing imagery is only of secondary importance. This is particularly the case for the geological, geomorphological, and soil data layers. The soil depth and slope hydrology information, which are very important in physical modeling of slope stability are also the most difficult to obtain, and remote sensing has not proven to be a very important tool for these. On the other hand, however, there are also data layers for which remote sensing data can be the main source of information. This is particularly so for landslide inventories, digital elevation models, and land use maps.

In the following sections an overview is given of the methods for spatial data collection. Most emphasis is given to landslide inventories, given their high importance, but also a number of aspects dealing with environmental factors, triggering factors and elements at risk will be discussed and illustrated.

3. Landslide inventory mapping

In order to make a reliable map that predicts the landslide hazard and risk in a certain area, it is crucial to have insight in the spatial and temporal frequency of landslides, and therefore each landslide hazard or risk study should start by making a landslide inventory that is as complete as possible in both space and time (Ibsen and Brunsden, 1996; Lang et al., 1999; Glade, 2001). Attempts have been made to standardize classification in nomenclature for landslides (IAEG-Commission on Landslides, 1990; UNESCO-WP/WLI, 1993a; Cruden and Varnes, 1996), landslide activity (UNESCO-WP/WLI, 1993b), causes of landslides (UNESCO-WP/WLI, 1994), rate of movement (IUGS-Working group on landslide, 1995) and remedial measures for landslides (IUGS-Working group on landslide, 2001). Landslide inventories can be carried out using a variety of techniques, which are summarized in Table 2.

3.1. Visual interpretation

For visual interpretation of landslides, stereoscopic imagery with a high to very high resolution is required (Mantovani et al., 1996; Metternicht et al., 2005). Optical images with resolutions larger than 3 m (e.g. SPOT, LANDSAT, ASTER, IRS-1D), as well as SAR images (RADARSAT, ERS, JERS, ENVISAT) have proven to be useful for visual interpretation of large landslides in individual cases (Singhroy, 2005), but not for landslide mapping on the basis of landform analysis over large areas.

Very high resolution imagery (QuickBird, IKONOS, CARTOSAT-1, CARTOSAT-2) has become the best option now for landslide mapping from satellite images (IGOS, 2003), and the number of operational sensors with similar characteristics is growing year by year, as more countries are launching earth observation satellites with stereo capabilities and resolution of 3 m or better. The high costs may still be a limitation for obtaining these very high resolution images for particular study areas, especially for multiple dates after the occurrence of main triggering events

Please cite this article as: van Westen, C.J., et al., Spatial data for landslide susceptibility, hazard, and vulnerability assessment: An overview, Engineering Geology (2008), doi:10.1016/j.enggeo.2008.03.010

Table 2
Overview of techniques for the collection of landslide information

Group	Technique	Description	Scale			
			Regional	Medium	Large	Detailed
Image interpretation	Stereo aerial photographs	Analog format or digital image interpretation with single or multi-temporal data set	M	H	H	H
	High Resolution satellite images	With monoscopic or stereoscopic images, and single or multi-temporal data set	M	H	H	H
	LiDAR shaded relief maps	Single or multi-temporal data set from bare earth model.	L	M	H	H
	Radar images	Single data set	L	M	M	M
(Semi) automated classification based on spectral characteristics	Aerial photographs	Image ratioing, thresholding	M	H	H	H
	Medium resolution multi spectral images	Single data images, with pixel based image classification or image segmentation	H	H	H	M
		Multiple date images, with pixel based image classification or image segmentation	H	H	H	M
	Using combinations of optical and radar data	Either use image fusion techniques or multi-sensor image classification, either pixel based or object based	M	M	M	M
(Semi) automated classification based on altitude characteristics	InSAR	Radar Interferometry for information over larger areas	M	M	M	M
		Permanent scatterers for pointwise displacement data	H	H	H	H
	LiDAR	Overlaying of LiDAR DEMs from different periods	L	L	M	H
	Photogrammetry	Overlaying of DEMs from airphotos or high resolution satellite images for different periods	L	M	H	H
Field investigation methods	Field mapping	Conventional method	M	H	H	H
		Using Mobile GIS and GPS for attribute data collection	L	H	H	H
	Interviews	Using questionnaires, workshops etc.	L	M	H	H
Archive studies	Newspaper archives	Historic study of newspaper, books and other archives	H	H	H	H
	Road maintenance organizations	Relate maintenance information along linear features with possible cause by landslides	L	M	H	H
	Fire brigade/police	Extracting landslide occurrence from logbooks on accidents	L	M	H	H
Dating methods for landslides	Direct dating method	Dendrochronology, radiocarbon dating etc.	L	L	L	M
	Indirect dating methods	Pollen analysis, lichenometry and other indirect methods,	L	L	L	L
Monitoring networks	Extensometer etc.	Continuous information on movement velocity using extensometers, surface tiltmeters, inclinometers, piezometers	–	–	L	H
	EDM	Network of Electronic Distance Measurements, repeated regularly	–	–	L	H
	GPS	Network of Differential GPS measurements, repeated regularly	–	–	L	H
	Total stations	Network of theodolite measurements, repeated regularly	–	–	L	H
	Ground-based InSAR	Using ground-based radar with slide rail, repeated regularly	–	–	L	H
	Terrestrial LiDAR	Using terrestrial laser scanning, repeated regularly	–	–	L	H

Indicated is the applicability of each technique for small, medium, large and detailed mapping scales. (H=highly applicable, M=moderately applicable, and L=Less applicable).

such as tropical storms or cyclones. Fig. 2 gives an example of the use of different types of imagery for landslide mapping in Tegucigalpa, Honduras.

Another interesting development is the visual interpretation of landslide phenomena from shaded relief images produced from LiDAR DEMs, from which the objects on the earth surface have been removed; so-called bare earth DEMs (Haugerud et al., 2003; Schulz, 2004). The use of shaded relief images of LiDAR DEMs also allows a much more detailed interpretation of the landslide mechanism as the deformation features within the large landslide are visible, and landslide can be mapped in heavily forested areas (Haneberg, 2004). Fig. 2H gives an example of the use of LiDAR for landslide mapping in Tegucigalpa, Honduras (Gutierrez et al., 2001).

However, in practice, aerial photo interpretation still remains the most used technique for landslide mapping (Tribe and Leir, 2004; Metternicht et al., 2005). Cardinali et al., 2002 present a clear example on the use of multi-temporal airphoto interpretation for the generation of a landslide database that can be used in landslide hazard and risk assessment. An analysis of the magnitude–frequency relationship based on landslide interpretations from multi-temporal airphotos has been carried out by Reid and Page (2002).

The conversion from conventional landslide inventory interpretations from stereoscopic aerial photographs to a GIS was rather time consuming. Nowadays the interpretation of stereo images can be done digitally, using two scanned stereo images, or one image combined with a DEM to produce an artificial stereo image. (Van Westen, 2004).

3.2. Automated landslide mapping

Many developments have taken place in the last decade related to methods for the automatic detection of landslides based on their spectral or altitude characteristics. The automatic characterization of landslide areas can make use of a number of features (Soeters and Van Westen, 1996):

- Disrupted or absent vegetation cover, anomalous with the surrounding terrain has been used as the main diagnostic feature for the recognition of landslides from multi-spectral images.
- Slope characteristics, related to the overall slope changes, and the presence of slope concavities and breaks of slope that might be recognizable from DEMs.
- Surface characteristics, such as internal deformation structures, fissures, tension cracks, flow lobes, step like morphology, scarps, and semi circular features are detectable as increased surface roughness, if the detail of the DEM is sufficiently large.
- Surface drainage characteristics, such as disrupted drainage, ponds, seepage zones, and exceptionally wet or dry zones might be detected using radar imagery or using thermal imagery.

Multi-spectral images such as SPOT, LANDSAT, ASTER and IRS-1D LISS3 have proven to be more applicable for landslide mapping based on image classification in conditions where landslides are fresh and unvegetated (Cheng et al., 2004).

Interesting examples of the use of optical satellite data for landslide inventory mapping are presented by Roessner et al. (2005), Nichol and Wong (2005). Restrepo and Alvarez (2006) demonstrated that image classification of multi-spectral images for landslide studies can be successful for identifying a large number of unvegetated scarps that have been produced during a single triggering event. However, practice has shown that the use of optical satellite imagery for multi-temporal landslide detection after major triggering events, especially in tropical areas, is often hampered by the persistent cloud cover in the affected

Please cite this article as: van Westen, C.J., et al., Spatial data for landslide susceptibility, hazard, and vulnerability assessment: An overview, Engineering Geology (2008), doi:10.1016/j.enggeo.2008.03.010

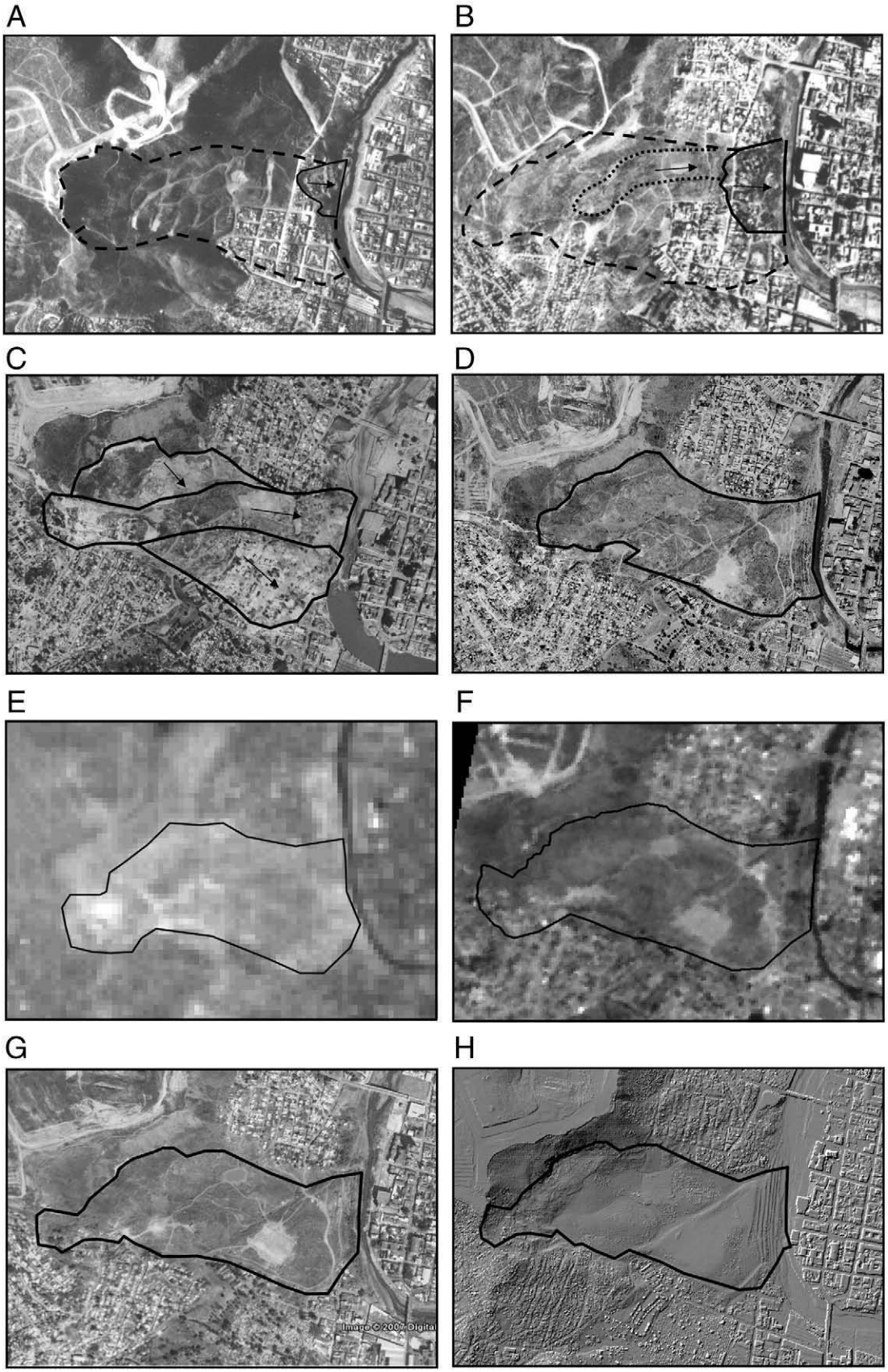

Fig. 2. Examples of different types of optical remote sensing images for El Berrinche landslide in Tegucigalpa, Honduras. A: Section of an Aerial photo, scale 1:14,000 from 16-March-1975, B: Section of an aerial photo, scale 1:20,000 from 9-February-1990, C: Section of an aerial photo, scale 1:25,000 from 1998, taken after hurricane Mitch, D: Section of an orthophoto, generated from 1:10,000 photos from May 2001, E: Section of a Aster image, with a spatial resolution of 15 m from 2005; F: Section of a IRS P6 image, with a spatial resolution of 5.6 m from 14-April 2006; G: Section of a Digital Globe image from Google Earth, from 2007; H: Shaded relief image from a LiDAR DEM with 1.5 meter spatial resolution.

Please cite this article as: van Westen, C.J., et al., Spatial data for landslide susceptibility, hazard, and vulnerability assessment: An overview, Engineering Geology (2008), doi:10.1016/j.enggeo.2008.03.010

area, which makes it difficult to obtain cloud-free images for a long period of time.

Automatic classification of landslides using digital airphotos has also been applied successfully by Hervas et al. (2003). Whitworth et al. (2005) have demonstrated the use of a high resolution Airborne Thermal Mapper (ATM) sensor with image processing for semi-automated landslide identification. Airborne hyperspectral imagery has been used as well in landslide mapping (Bianchi et al., 1999). Image classification methods used for landslide mapping can be differentiated in pixel based and non-pixel based ones. Currently, non-pixel based approaches using object oriented image segmentation seem to provide a better accuracy than pixel based methods (Barlow et al., 2003; Martin and Franklin, 2005).

Many methods for landslide mapping make use of digital elevation models of the same area from two different periods. The subtraction of the DEMs allows visualizing where displacement due to landslides has taken place, and the quantification of displacement volumes (Oka, 1998; Van Westen and Getahun, 2003; Dewitte and Demoulin, 2005). Satellite derived DEMS from SRTM, ASTER and SPOT do not provide sufficient accuracy to differentiate actual landslide movement from noise, when overlaying two DEMs from different dates (Hirano et al., 2003). High resolution data from Quickbird, IKONOS, PRISM (ALOS) and CARTOSAT-1 are able to produce highly accurate digital elevation models that might be useful in automatic detection of large and moderately large landslides.

Light Detection and Ranging (LiDAR) or laser scanning can provide high resolution topographic information (<1 m horizontal and a few cm vertical accuracy), depending on the flying height, point spacing and type of terrain, and may be as low as 100 cm in difficult terrain (Haneberg, 2004; McKean and Roering, 2004; Glenn et al., 2006). Also the combination of an Airborne Laser Scanner (ALS) and Terrestrial Laser Scanner (TLS) for the quantification of landslide volumes has been proven successfully (Hsiao et al., 2004). Terrestrial LiDAR measurements have also been successfully applied for the monitoring of individual landslide by Rowlands et al. (2003) and Jones (2006).

Interferometric Synthetic Aperture Radar (InSAR) has been used extensively for measuring surface displacements. Unfortunately, in most environments InSAR applications are limited by problems related to geometric noise due to the different look angles of the two satellite passes and temporal de-correlation of the signal due to scattering characteristics of vegetation, as well as by atmospheric variability in space and time (Catani et al., 2005; Reidel and Walther, 2008). To overcome these problems, the technique of Persistent Scatterer Interferometry (PSI), or Permanent Scatterers was introduced (Ferretti et al., 2001) that uses a large number of radar images and works as a time series analysis for a number of fixed points in the terrain with stable phase behavior over time, such as rocks or buildings. The availability of ERS-1 and 2, RADARSAT, together with the recent ENVISAT and ALOS PALSAR now offer many more opportunities for obtaining a large time series spanning 4 to 10 years (with 30–100 images). These techniques are only possible if the landslide displacement is not too much (in the order of centimeters), and therefore cannot be applied for mapping new landslides with a large displacement.

3.3. Generation of landslide databases

The techniques described above are intended to support the generation of landslide databases. Such databases may have a very large degree of uncertainty, which can be related to the incompleteness of historical information (with respect to the exact location, time of occurrence, and type of movement), or to the experience and dedication of the persons carrying out the image interpretation and field mapping (Soeters and Van Westen, 1996). The difficulties involved in obtaining a complete landslide database, and its implications for landslide hazard assessment are illustrated in Fig. 3. The graph indicates a hypothetical landslide frequency in the period 1960–2006, and the main triggering

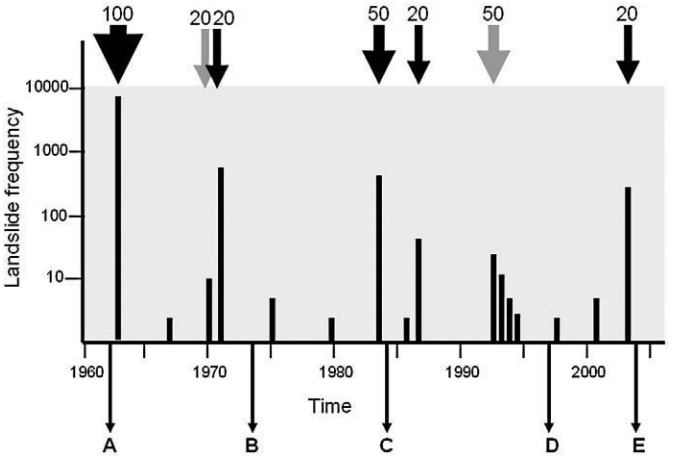

Fig. 3. Schematic presentation of landslide frequency in relation to triggering events and dates of imagery. On top of the graph the rainfall events (in black) and earthquakes (in gray) are indicated as arrows, with an indication of their return periods. The black arrows below the graph (A to E) refer to dates of available remote sensing imagery for landslide inventory mapping.

events (either earthquakes or rainfall events) with the return period indicated. For the area, five different sets of imagery are available (indicated in Fig. 3 with A to E). In order to be able to capture those landslides related with a particular triggering event, it is important to be able to map these as soon as possible after the event occurred. For example the imagery of C and E can be used to map the landslides triggered by rainfall events with different return periods. The imagery of B and D however, are taken either some time after the triggering event has occurred, so that landslide scarps will be covered by vegetation and are difficult to interpret, or they occur after a sequence of different triggering mechanisms, which would make it difficult to separate the landslide distributions. This is also illustrated for the Tegucigalpa area in Fig. 2, where the landslide inventory of past events is limited by the availability of historical imagery. For instance, if image C in Fig. 2 (taken directly after the occurrence of Hurricane Mitch) would not have been available, it would have been very difficult to identify the landslide type and mechanism on the later imagery (e.g. D).

This illustrates the importance of obtaining imagery as soon as possible after the occurrence of a major triggering event, so that accurate event-based landslide maps can be made, which in turn will make it possible to derive landslide probability maps. Such event-based landslide inventory maps should be stored in a landslide database implemented in GIS.

Much progress has been made in the development of landslide inventories at regional or national level. One of the first comprehensive projects for landslide and flood inventory mapping has been the AVI project in Italy (Guzzetti et al., 1994). Many countries are developing landslide databases through map servers on the Internet, for example in Hong Kong (CEDD, 2007), Canada (Grignon et al., 2004), Australia (Geoscience Australia, 2006), Japan (NIED, 2006), Norway (NGU, 2006), Italy (CNR-IRPI 2006), Nicaragua (INETER, 2006) and New Zealand (Glade and Crozier, 1996).

There are good examples in the literature of the use of landslide inventories for hazard assessment (Guzzetti et al., 1994; Guzzetti, 2000; Chau et al., 2004; Guzzetti and Tonelli, 2004). However, the existing landslide databases often present several drawbacks (Guzzetti, 2000; Ardizzone et al., 2002; Guzzetti and Tonelli, 2004) related to the completeness in space and even more so in time, and the fact that they are biased to landslides that have affected infrastructures such as roads.

3.4. Landslide inventory for Tegucigalpa

To illustrate some of the aspects discussed above in relation to landslide inventory mapping and the generation of landslide databases, an

Please cite this article as: van Westen, C.J., et al., Spatial data for landslide susceptibility, hazard, and vulnerability assessment: An overview, Engineering Geology (2008), doi:10.1016/j.enggeo.2008.03.010

example is given in Fig. 2 of a large landslide, named El Berrinche, in the centre of the city of Tegucigalpa, Honduras. This landslide occurred in late October 1998, as a result of heavy rainfall and undercutting of the toe by the Choluteca River, during the passing of hurricane Mitch (Peñalba et al., 2007). Tegucigalpa is located in a bowl shaped valley of the Choluteca River, underlain in the SE by Cretaceous Rio Chiquito

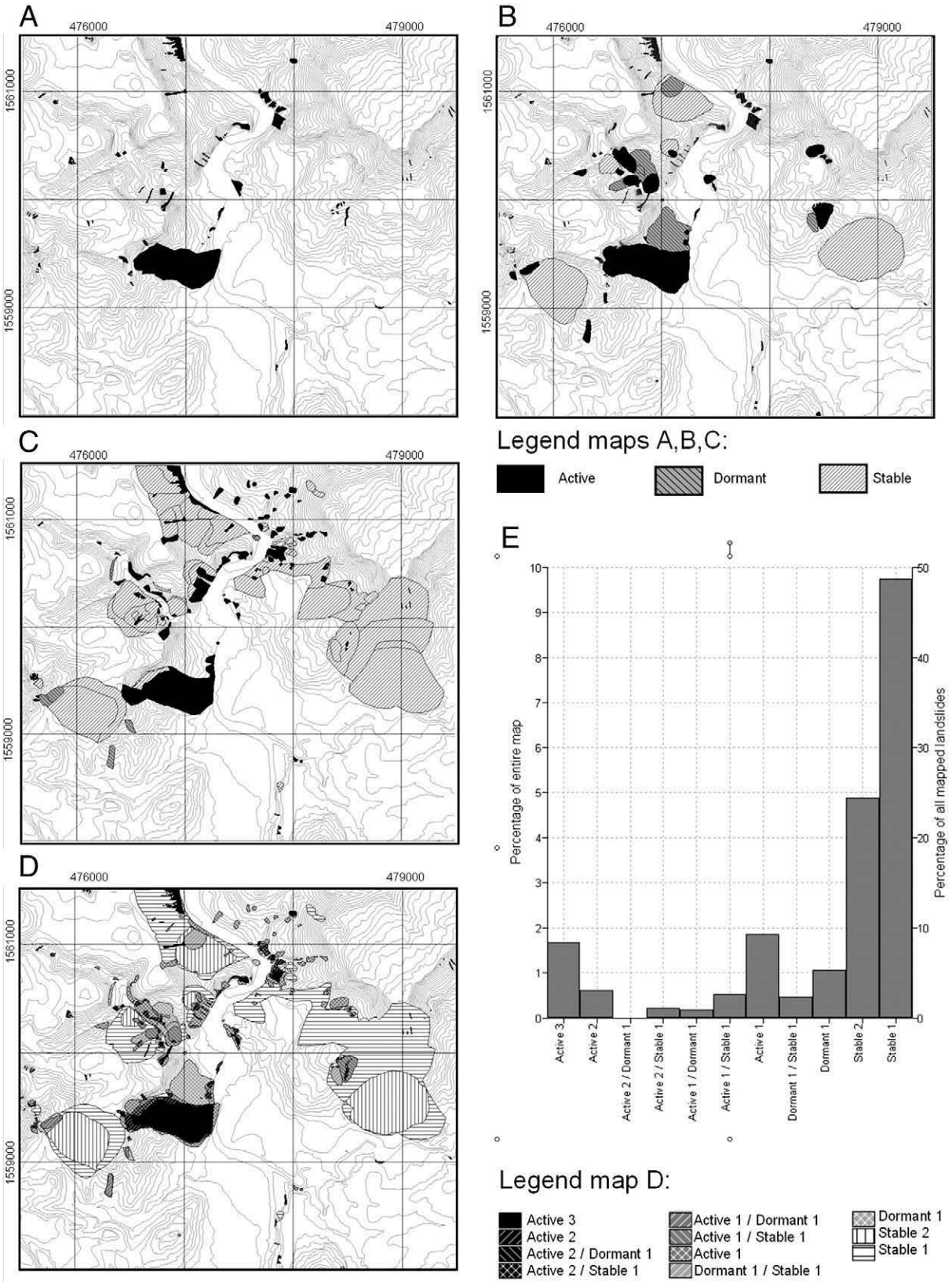

Fig. 4. Three landslide inventory maps generated after hurricane Mitch. A: Inventory map of the first mapping source, in which only the landslide caused by Mitch have been mapped, B: Landslide inventory map generated by the second source, in which also a number of older landslides have been recognized, C: Landslide inventory of source three, in which image interpretation of old airphotos revealed the occurrence of many paleo-landslides, D: Combination of the three inventory maps, E: Histogram of the combined map D.

Please cite this article as: van Westen, C.J., et al., Spatial data for landslide susceptibility, hazard, and vulnerability assessment: An overview, Engineering Geology (2008), doi:10.1016/j.enggeo.2008.03.010

formation, consisting of red sandstone, siltstone and some conglomerates, and Tertiary volcanic deposits in the northwestern part (Rogers and O'Conner, 1993). The highest parts of the area are plateaus underlain by ignimbrites with steep cliffs around their edges and a complex series of old landslides, which have not been dated till now. One of these is the El Berrinche landslide (see Fig. 2), which is approximately 700 meter long and 400 meter wide. The landslide has had several phases of activity over the last decades, which culminated in the massive failure on October 31 1998 (Peñalba et al., 2007). The movement history can be reconstructed with the help of image interpretation, utilizing aerial photographs, satellite images and LiDAR data from different periods. As can be seen in Fig. 2A, which is an airphoto from 1974, the landslide can be clearly recognized, and a reactivation which occurred in the toe of the landslide in 1970 is evident. During this period also the houses of the Colonia Soto were already constructed on the landslide, and the road construction in the higher parts suggests that further development was planned, which was never implemented, due to the landslide movements. A second reactivation took place in 1984, which produced considerable damage to roads and houses in the area (See Fig. 2B). The first signs of what later would form into an earthflow can be identified on the aerial photo from 1990, as well as the depressions in the upper part of the landslide. After a geotechnical investigation the area was declared unsafe and further development was not considered appropriate. The main movement occurred in October 1998, and the aerial photo taken just after this (Fig. 2C) clearly shows the different components of the landslide consisting of a rotational block in the upper part, an earthflow in the center and a compressional toe (Olsen and Villanueva, 2007). The landslide had a volume of 6 million cubic meters, and most of houses of the Colonia Soto were ruined as well as parts of the adjacent neighbourhoods. The landslide dammed the Choluteca River leading to extensive flooding in the center of Tegucigalpa for a number of weeks. After the event the slope was flattened and a series of benches were constructed along the toe (See Fig. 2D). Also a drainage diversion channel was constructed in a SW–NE direction. Fig. 2E, F and G show satellite imagery for the same area from subsequent years (Aster image from 2005, IRS-P6 image from 2006 and Digital Globe image from Google Earth taken in 2007) on which no major changes can be identified. The figure also shows that only very high resolution imagery, with spatial resolution of 1 m or higher allows proper interpretation of landslide phenomena. It should be noted here also that the use of stereo images is essential, as many of the diagnostic features related to morphology can only be interpreted in three-dimensions. Finally, Fig. 2H illustrates the applicability of LiDAR shaded relief maps for the interpretation of the landslide components (Gutierrez et al., 2001; Harp et al., 2002a).

The landslides caused by Hurricane Mitch were mapped by several teams (Harp et al., 2002a; JICA, 2002). Fig. 4 gives three landslide inventory maps for the area around the centre of Tegucigalpa, taken from three independent sources. Map A was made using field investigation directly after the occurrence of Mitch. Map B was made a few years later, based on field investigations and aerial photo interpretation, using photographs taken directly after the event. Map C was made 6 years later, based only on aerial photo interpretation, using different sets of aerial photographs, from 1975, 1990 and from 2000. Fig. 4D and E show the overlap of the three landslide inventory maps, while Table 3 shows the specific combinations. There is a considerable variation among the three landslide maps, both in terms of the location of the events, as well as their classification. Here only the classification of the activity is given. Of all the landslides mapped by the three groups only 10% was mapped similarly. These were also the active landslides that were produced directly after hurricane Mitch. However, of the active landslides identified by one of the three sources, only 33% was mapped similarly by all, and 50% was mapped by only one of the three sources. As Map A didn't consider dormant and stable landslides, it is difficult to compare these types for the three maps. However, the largest differences are caused by the mapping of old landslides, which are now considered to be stable. Map B and Map C differ quite substantially in their interpretation of these older events. The mapping of these older events is very important, as it helps to identify reactivation hazard, clearly demonstrated by the El Berrinche landslide. Although the maps in Fig. 4 only present the landslide activity, information was also collected on the landslide types and depths, and the components of the landslide (scarp area, transport zone, accumulation area).

Table 3
Comparison of three landslide inventory maps generated after hurricane Mitch, shown in Fig. 4

Map A	Map B				
	Active	Dormant	Stable	None	Total
Active	2.118	0.000	0.000	0.146	2.26
Dormant	0.000	0.000	0.000	0.000	0.00
Stable	0.000	0.000	0.000	0.000	0.00
None	1.566	1.421	5.322	89.426	97.74
Total	3.68	1.42	5.32	89.57	100.00
Map C	Map B				
	Active	Dormant	Stable	None	Total
Active	1.986	0.074	0.052	1.074	3.19
Dormant	0.166	0.000	0.074	0.137	0.38
Stable	0.669	0.424	4.882	9.388	15.36
None	0.864	0.923	0.358	78.929	81.07
Total	3.68	1.42	5.37	89.53	100.00
Map C	Map A				
	Active	Dormant	Stable	None	Total
Active	1.681	0.000	0.000	1.505	3.19
Dormant	0.000	0.000	0.000	0.334	0.33
Stable	0.206	0.000	0.000	15.157	15.36
None	0.377	0.000	0.000	80.740	81.12
Total	2.26	0.00	0.00	97.74	100.00

The values show the percentage of the entire area.

The large differences between the landslide inventory maps illustrate the high degree of uncertainty of this very important input data layer for landslide susceptibility, hazard and risk assessment. The difference in landslide patterns will have a very large effect on the subsequent landslide susceptibility mapping, especially when statistical methods are used. It is therefore important to both map event-based landslide inventory maps, as well as map older landslides, and includes a proper interpretation of the landslide types, failure mechanisms and (relative) dates.

4. Environmental factors

As indicated in Fig. 1, the next block of spatial information required for landslide susceptibility, hazard and risk assessment consists of the spatial representation of the factors that are considered relevant for the prediction of the occurrence of future landslides. Table 4 provides more details on the relevance of these factors for heuristic, statistical and deterministic analysis. It is clear from this table that the three types of analysis use different types of data, although they share also common ones, such as slope gradient, soil and rock types, and land use types. The selection of the environmental factors that are used in the susceptibility assessment is depending on the type of landslide, the type of terrain and the availability of existing data and resources. A good understanding of the different failure mechanisms is essential. Often different combinations of environmental factors should be used, resulting in separate landslide susceptibility maps for each failure mechanism. Below, some of the environmental factors are discussed in more detail.

4.1. Digital elevation data

As topography is one of the major factors in landslide hazard analysis, the generation of a digital representation of the surface

Please cite this article as: van Westen, C.J., et al., Spatial data for landslide susceptibility, hazard, and vulnerability assessment: An overview, Engineering Geology (2008), doi:10.1016/j.enggeo.2008.03.010

Table 4
Overview of environmental factors, and their relevance for landslide susceptibility and hazard assessment

Group	Data layer and types	Relevance for landslide susceptibility and hazard assessment	Scales of analysis			
			Regional	Medium	Large	Detailed
Digital elevation models	Slope gradient	Most important factor in gravitational movements	L	H	H	H
	Slope direction	Might reflect differences in soil moisture and vegetation	H	H	H	H
	Slope length/shape	Indicator for slope hydrology	M	H	H	H
	Flow direction	Used in slope hydrological modeling	L	M	H	H
	Flow accumulation	Used in slope hydrological modeling	L	M	H	H
	Internal relief	Used in small scale assessment as indicator for type of terrain.	H	M	L	L
	Drainage density	Used in small scale assessment as indicator for type of terrain.	H	M	L	L
Geology	Rock types	Lithological map based on engineering characteristics rather than on stratigraphic classification.	H	H	H	H
	Weathering	Depth of weathering profile is an important factor for landslides	L	M	H	H
	Discontinuities	Discontinuity sets and characteristics relevant for rock slides	L	M	H	H
	Structural aspects	Geological structure in relation with slope angle and direction is relevant for predicting rock slides.	H	H	H	H
	Faults	Distance from active faults or width of fault zones is important factor for predictive mapping.	H	H	H	H
Soils	Soil types	Engineering soil types, based on genetic or geotechnical classification	M	H	H	H
	Soil depth	Soil depth based on boreholes, geophysics and outcrops is crucial data layer in stability analysis	L	M	H	H
	Geotechnical properties	Grain size distribution, cohesion, friction angle, bulk density are the crucial parameters for slope stability analysis	L	M	H	H
	Hydrological properties	Pore volume, saturated conductivity, PF curve are the main parameters used in groundwater modeling	L	M	H	H
Hydrology	Water table	Spatially and temporal varying depth to ground water table	L	L	M	H
	Soil moisture	Spatially and temporal varying soil moisture content is one of main components in stability analysis	L	L	M	H
	Hydrologic components	Interception, Evapotranspiration, throughfall, overland flow, infiltration, percolation etc.	M	H	H	H
	Stream network	Buffer zones around first order streams, or buffers around eroding rivers	H	H	H	L
Geomorphology	Physiographic units	Gives a first subdivision of the terrain in zones, which is relevant for small scale mapping	H	M	L	L
	Terrain Mapping Units	Homogeneous units with respect to lithology, morphography and processes	H	M	L	L
	Geomorphological units	Genetic classification of main landform building processes, their	H	H	M	L
	Geomorphological (sub)units	Geomorphological subdivision of the terrain in smallest units, also called slope facets	H	H	H	L
Landuse	Land use map	Type of land use/land cover is a main components in stability analysis	H	H	H	H
	Land use changes	Temporal varying land use/land cover is a main components in stability analysis	M	H	H	H
	Vegetation characteristics	Vegetation type, canopy cover, rooting depth, root cohesion, weight etc.	L	M	H	H
	Roads	Buffers around roads in sloping areas with road cuts are often used as factor maps.	M	H	H	H
	Buildings	Areas with slope cuts made for building construction are sometimes used as factor	M	H	H	H

(H = highly applicable, M = moderately applicable, and L = Less applicable). Adapted from Soeters and van Westen (1996).

elevation, called Digital Elevation Model (DEM), plays a major role. Digital Elevation Models (DEMs) can be derived through a large variety of techniques, such as digitizing contours from existing topographic maps, topographic leveling, EDM (Electronic Distance Measurement), differential GPS measurements, (digital) photogrammetry, InSAR, and LiDAR. Traditionally the most used method for the generation of DEMs as input maps in landslide hazard assessment was the digitizing of contourlines from topographic maps, and the subsequent interpolation into either raster or vector (Triangular Irregular Networks) DEMs. The accuracy of the resulting DEM depends on the scale of the input map, the contour interval, the availability of additional spotheight information, the precision of digitizing, and the interpolation method used. For detailed measurement of small areas Differential Global Positioning Systems (DGPS) utilize correction signals sent to a single GPS receiver to achieve submeter horizontal accuracy and vertical accuracy in the one to three meter range. During the last 15 years there have been important changes both in terms of data availability, as well as in terms of software that can be used on normal desktop computers, without extensive skills in photogrammetry. Nowadays, Digital Photogrammetry can be used on desktop computers on a variety of images, ranging from metric air photographs taken on official surveys from National Mapping Agencies, to small format photography taken from helicopters, light aircraft and drones (Henry et al., 2002).

Global DEMs are available with a horizontal grid spacing ranging from 30 arc sec (approximately 1 km), such as GLOBE or GTOPO30 (Hastings and Dunbar, 1998), to 5-arc-minute spatial resolution (e.g. ETOPO5, TerrainBase and JGP95E), or larger (e.g. ETOPO2). In terms of satellite derived DEMs, the NASA Shuttle Radar Topography Mission (SRTM) has gathered topographic data for about 80% of the Earth's land surface, in the area between 60° latitude (Rabus et al., 2003). The released SRTM DEMs for the United States are at 30 meter resolution, and those for the rest of the world at 90 m. SRTM data often has a problem with missing data, and the vertical error can be up to 15 m in mountainous areas (Farr et al., 2007).

These days a wide range of data sources can be selected for the generation of DEMs (see Table 5). The selection depends on the data availability for a specific area, the price and the application. Optical images with 5–15 meter spatial resolution (e.g. IRS-1C and 1D, SPOT-5/HRS, SPOT-2-4/HRV, ASTER) in particular are suitable for medium scale mapping, and some are also relatively low priced. As mentioned before, ASTER scenes are particularly affordable (<55 USD per scene of 60 by 60 km) and produce DEMs with spatial resolution of 15 m and vertical accuracy of 20 m (Fujisada et al., 2005). The application of

Please cite this article as: van Westen, C.J., et al., Spatial data for landslide susceptibility, hazard, and vulnerability assessment: An overview, Engineering Geology (2008), doi:10.1016/j.enggeo.2008.03.010

Table 5
Main sources for digital elevation models used in landslide hazard and risk assessment studies, and their application in the four defined mapping scales, (TG: too general, as the data is not sufficiently detailed for the mapping scale, TD: too detailed, and data collection too costly given the relatively low requirements at the given scale)

Method	Examples	Scale of analysis			
		Small	Medium	Large	Detailed
Global DEMs	ETOPO2 (1.86 km pixel)	Hillshading Physiography Internal relief Drainage density	TG	TG	TG
Contour map derived DEMs	1:100,000 (40 m cont.int)	Hillshading Physiography Internal relief Drainage density	TG	TG	TG
	1:25,000 (10 m cont.int)	Hillshading Physiography Internal relief Drainage density	DEM derivatives: slope steepness, aspect, length, convexity etc.	TG	TG
	1:10,000 (5 m cont.int)	TD	DEM derivatives: slope steepness, aspect, length, convexity etc.	Slope angles Flow accumulation Run out modeling	TG
	1:5000 (2 m cont.int)	TD	TD	Slope angles Flow accumulation Run out modeling	Slope angles Flow accumulation Run out modeling
Medium resolution Satellite derived DEMS	SRTM (30–90 m pixel)	Hillshading Physiography Internal relief Drainage density	TG	TG	TG
	ASTER (15 m pixel)	Hillshading Physiography Internal relief Drainage density	DEM derivatives: slope steepness, aspect, length, convexity etc.	TG	TG
High Resolution Satellite derived DEMs	Quickbird, IKONOS (1–4 m)	TD	DEM derivatives: slope steepness, aspect, length, convexity etc.	Slope angles Flow accumulation Run out modeling Change detection	Slope angles Flow accumulation Run out modeling Change detection
	PRISM, CARTOSAT (2.5 m)	TD	DEM derivatives: slope steepness, aspect, length, convexity etc.	Change detection Slope angles Flow accumulation Run out modeling	Change detection Slope angles Flow accumulation Run out modeling
InSAR	RADARASAT, ENVISAT etc.	TD	Landslide monitoring Change detection	Landslide monitoring Change detection	Landslide monitoring Change detection
LiDAR	ALTM, ALS (1 m DEM)	TD	DEM derivatives: slope steepness, aspect, length, convexity etc. Run out modeling DSM Building extraction	Landslide monitoring Slope angles Flow accumulation Run out modeling DSM Building extraction	Landslide monitoring Slope angles Flow accumulation Run out DSM Building extraction

DEMs from very high resolution images (Quickbird or IKONOS) in landslide studies is hampered by the high acquisition costs (30–50 USD/km^2). The recently launched high resolution data from PRISM (ALOS) and CARTOSAT-1, both with 2.5 m resolution, and two panchromatic cameras that allow for near simultaneous imaging of the same area from two different angles (along track stereo) are able to produce highly accurate Digital Elevation Models, at expected lower costs than 10 USD/km^2. Although Radar Interferometry is used for landslide change detection, it is not used extensively for DEM generation as a factor map in landslide studies, mostly because of problems with vegetation.

Light Detection And Ranging (LiDAR) is a relatively new technological tool, which is very useful for terrain mapping. Normally LiDAR point measurements will render so-called Digital Surface Models (DSM), which contains information on all objects of the Earth's surface, including buildings, trees etc., (Ackermann, 1999). Through sophisticated algorithms, and final manual editing, the landscape elements are removed and a Digital Terrain Model is generated. The difference between a DSM and the DTM can also provide very useful information, e.g., on elements at risk (buildings etc. see later section) or the forest canopy height. LiDAR has become the standard method for the generation of DEMs in many developed countries already and it is likely that most countries will be having LiDAR derived DEMs within a decade or so. The average costs of LiDAR ranges from 300–800 USD/km^2 depending on the required point density.

Many derivate maps can be produced from DEMs using fairly simple GIS operations (Moore et al., 2001). This might also be the reason why so many landslide hazard studies include derivative maps such as slope aspect in the landslide hazard analysis, even though the exact relation between slope aspect and landslide occurrence is not always clear. Derivatives from DEMs can be used in heuristic analysis at small scales (hillshading images for display as backdrop image, physiographic classification, internal relief, drainage density), in statistical analysis at medium scales (e.g. altitude zones, slope gradient, slope direction, contributing area, plan curvature, profile curvature, slope length), in deterministic modeling at large scales (local drain direction, flow path, slope gradient) and in landslide run out modeling (detailed slope morphology, flow path, rock fall movement) (e.g. Corominas et al., 1992). An example of DEM derivatives obtained from an SRTM DEM for the watershed area of the Choluteca River in Honduras is presented in Fig. 5.

Although there are many DEM derived maps that can be produced not all of them are suitable for landslide susceptibility assessment and

Please cite this article as: van Westen, C.J., et al., Spatial data for landslide susceptibility, hazard, and vulnerability assessment: An overview, Engineering Geology (2008), doi:10.1016/j.enggeo.2008.03.010

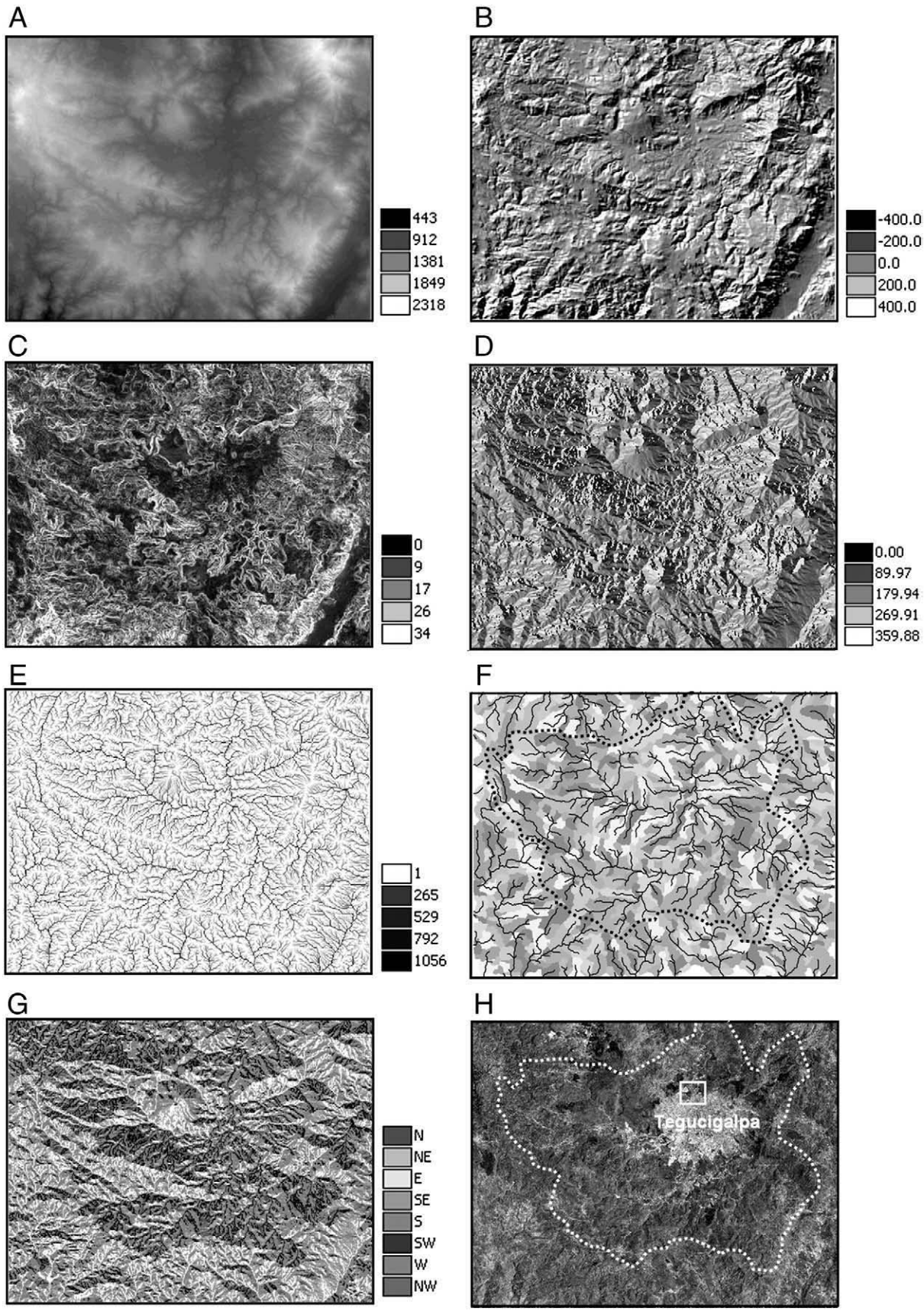

Fig. 5. Examples of derivative maps from a SRTM DEM of the watershed of the Choluteca River, near Tegucigalpa. A: Altitude, B: Shaded relief image, C: Slope angle (in degrees), D: Slope direction (in degrees), E: Flow accumulation, F: Automatic drainage and catchment delineation, G: Drainage direction, H: Landsat TM image showing the location of Tegucigalpa, and the watershed boundary.

Please cite this article as: van Westen, C.J., et al., Spatial data for landslide susceptibility, hazard, and vulnerability assessment: An overview, Engineering Geology (2008), doi:10.1016/j.enggeo.2008.03.010

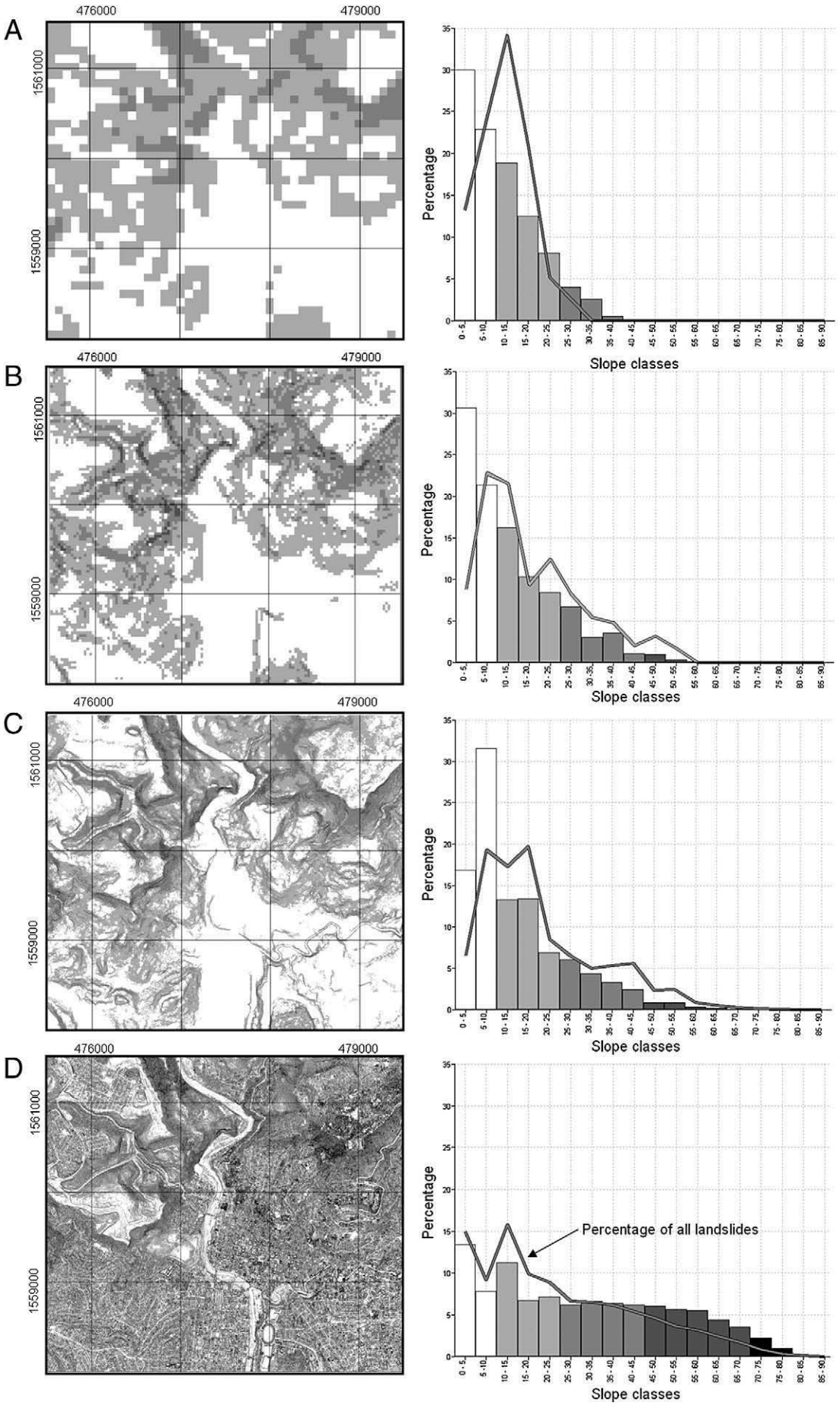

Please cite this article as: van Westen, C.J., et al., Spatial data for landslide susceptibility, hazard, and vulnerability assessment: An overview, Engineering Geology (2008), doi:10.1016/j.enggeo.2008.03.010

also not at all scales. Zhou and Liu (2004) present a detailed investigation of the accuracy of slope and aspect maps derived from DEMs with different resolutions. Scale limitation of models due to DEM resolution has been studied for other types of model like soil erosion but little research has been carried out on this issue for landslide hazard and risk assessment models (Dietrich and Montgomery, 1998). Claessens et al. (2005) conclude that the variable gridsizes of raster DEMs used in deterministic slope stability assessment have a large effect on the distribution of areas modeled as unstable. Also the use of slope gradient maps in statistical landslide hazard assessment is greatly affected by differences in the resolution of the DEM and the derived slope maps. As a general rule of thumb the use of slope gradient maps is not advisable for small scale studies, whereas in medium scale studies slope maps, and other DEM derivatives such as aspect, slope length, slope shape etc. can be used as input factors for heuristic or statistical analysis. In large and detailed scale hazard assessment, DEMs is used in slope hydrology modeling and slope maps are used for deterministic slope stability modeling (see Table 4). On the other hand, also the use of high accurate LiDAR DEMs poses some problems. The high spatial resolution of a LiDAR data set often doesn't match with the detail of the other environmental factors, and the very local variations in slope angle depicted in the LiDAR DEM might not be representative of the more general slope conditions under which landslides might occur.

4.2. Example of the use of DEMs in Tegucigalpa

To illustrate some of the points indicated above on the use of Digital Elevation Models, Figs. 5 and 6 shows the use of different DEMs for the case study area in Honduras. Fig. 5 shows a series of derivative maps generated from the SRTM DEM with 90 meter spatial resolution. After obtaining the raw data, several processing steps had to be applied in order to correct for the missing data values and to remove so-called “sinks”, which are closed depression in the DEM due to artifacts. The resulting DEM derivatives were successfully used in a regional landslide susceptibility assessment using statistical analysis, together with other environmental factors, as mentioned in Table 4. The LiDAR DEM was also utilized for generation of a susceptibility map, using a soil water model combined with an infinite slope model to produce a factor of safety map by Harp et al. (2002b).

The LiDAR DEM of the Tegucigalpa area was obtained from the USGS. It was collected by the University of Texas using an ALTM 1225 in March 2000, at an altitude of 800–1200 resulting in a spacing of 2.6 m between scan lines (Gutierrez et al., 2001). A TopScan vegetation removal filter was applied and the data was interpolated into a 1.5 meter resolution DEM. The LiDAR DEM was used together with the SRTM DEM (90 meter spatial resolution) and with two other DEMS from contour maps. The first contour maps had a scale of 1:2000, 2.5 m contour lines and the resulting DEM was made at 1 meter spatial resolution. The second contour map was at scale 1:50,000 with 20 meter contour lines interpolated in a DEM with 30 meter pixelsize. The four DEMs were used to produce slope angle maps, using horizontal and vertical gradient filters. The resulting slope maps were classified into classes of 10°, and overlain with the landslide inventory map of the Mitch landslides (Map A in Fig. 4). Fig. 6 shows the 4 slope class maps with the corresponding histograms. The slope class maps derived from SRTM and 1:50,000 scale topomaps contain more flat areas as compared to the DEMs from 1:2000 topomaps and LiDAR. The landslide–slope class relationship is also substantially different. There is a large difference between the LiDAR DEM and the DEM from the detailed topomap, due to the inclusion of buildings in this DEM. From the figure it can be concluded that the resolution and accuracy of the DEM has a very large influence on the relation between slope classes and landslides.

4.3. Geological and soil data

Traditionally, geological maps form a standard component in heuristic and statistical landslide hazard assessment methods. Mostly the stratigraphical legends of existing geological maps are converted into an engineering geological classification, which gives more information on the rock composition and rock mass strength (Carrara et al., 1999).

In medium and small scale analysis the subdivision of geological formations into meaningful mapping units of individual rock types often poses a problem, as the intercalations of these units cannot be properly mapped at these scales. In detailed hazard studies specific engineering geological maps are collected and rock types are characterized using field tests and laboratory measurements. For detailed analysis also 3-D geological maps have been used, although the amount of outcrop and borehole information collected will make it difficult to use this method on a scale smaller than 1:5000, and its use is restricted mostly to a site investigation level (e.g. Xie et al., 2003).

Apart from lithological information also structural information is very important for landslide hazard assessment, as the orientation of the discontinuities in the (weathered) rock in relation with the slope angle and direction are of large influence in the susceptibility to landslides. At medium and large scale attempts have been made to generate maps indicating dip direction and dip amount, based on field measurements, but the success of this depends very strongly on the amount of measurements and the complexity of the geological structure. Another option is to map the relation between slope gradient/slope direction and bedding slope/direction for individual slope facets (Atkinson and Massari, 1998; Lee et al., 2002). Fault information is also used frequently as one of the environmental factors in a statistical landslide hazard assessment. The use of wide buffer zones around faults, which is now the standard practice should be treated with caution, as this might be only true for active faults. In other cases a very narrow buffer zone should be taken, which is related to the zone where rocks are fractured.

In terms of soil information required for landslide hazard assessment, there are basically two different thematic data layers needed: soil types, with associated geotechnical and hydrological properties, and soil sequences, with depth information. These data layers are essential components for any deterministic modeling approach. Pedologic soil maps, normally only classify the soils based on the upper soil horizons, with rather complicated legends and are therefore less relevant in case of landslide deeper than 1–2 m. Engineering soil maps describe all loose materials on top of the bedrock, and classify them according to the geotechnical characteristics. They are based on outcrops, borehole information and geophysical studies. Especially the soil depth is very difficult to map over large areas, as it may vary locally quite significantly. Soil thickness can be modeled using a correlation with topographic factors such as slope (e.g. Salciarini et al., 2006), or predicted from a process based model (Casadei et al., 2003). Given the fact that soil thickness is one of the most crucial factors in deterministic slope stability modeling, it is

Fig. 6. Effect of the use of different DEMs on the relation between slope angle and landslide distribution. The left side of the figure shows the slope angle maps (in degrees) generated from: A. SRTM data; with 90 meter spatial resolution, B. 1:50,000 topomaps with 20 meter contour interval, resulting in a DEM with 30 m horizontal resolution, C. 1:2000 topomaps with 2.5 meter contour interval, resulting in a DEM with 1 meter spatial resolution, D. a LiDAR image, from which the vegetation has been removed, with 1.5 meter spatial resolution. The right side of the figure shows the percentage of area per slope class (bar charts), and the percentage of all landslides per slope class (thick lines).

Please cite this article as: van Westen, C.J., et al., Spatial data for landslide susceptibility, hazard, and vulnerability assessment: An overview, Engineering Geology (2008), doi:10.1016/j.enggeo.2008.03.010

surprising that very limited work has been done on the modeling of soil thicknesses over larger areas (Terlien et al., 1995; Dietrich et al., 1995).

Geological and soil data collection can be performed more efficiently with the use of mobile GIS. Several methods for digital field data collection have been developed, such as PenMap (Kramer, 2000) and the generic systems such as ArcPad from ESRI, which is the most convenient one when working with ArcGIS.

4.4. Geomorphological data

Geomorphological maps are made at various scales to show land units based on their shape, material, processes and genesis (e.g. Klimaszewski, 1982; De Graaff et al., 1987). There is no generally accepted legend for geomorphological maps, and there may be a large variation in contents based on the experience of the geomorphologist. These very detailed maps contain a wealth of information, but require extensive field mapping, and are very difficult to convert into digital format (Gustavsson et al., 2006). Unfortunately, the traditional geomorphological mapping seems to have nearly disappeared with the developments of digital techniques, and very few publications on landslide hazard and risk still include it (Castellanos and Van Westen, 2008), or replace it by merely morphometric information.

An important new field within geomorphology is the quantitative analysis of terrain forms from DEMs, called geomorphometry or digital terrain analysis, which combines elements from earth sciences, engineering, mathematics, statistics and computer science. (Rowbotham & Dudycha 1998; Wilson & Gallant 2000; Pike, 2000). Part of the work focuses on the automatic classification of geomorphological land units based on morphometric characteristics at small scales (Giles and Franklin, 1998; Miliaresis, 2001) or on the extraction of slope facets at medium scales which can be used as the basic mapping units in statistical analysis (Carrara et al., 1995). For example Asselen and Seijmonsbergen (2006) present a semi-automated method to recognize and spatially delineate geomorphological units in mountainous forested areas in Vorarlberg (Austria), using statistical information extracted from a 1-m resolution LiDAR data set.

In most of the statistical methods the analysis is carried out for a number of basic mapping units, that can be either grid cells, slope facets that are derived from DEMs (Rowbotham and Dudycha, 1998) or unique conditions units which are made by overlaying a number of landslide preparatory factors, such as lithology, land cover, slope gradient, slope curvature and upslope contributing area (Carrara et al., 1995).

4.5. Landuse data

Landuse is too often considered as a static factor in landslide hazard studies, and few researches involve constantly changing land use as a factor in the analysis (Van Beek and Van Asch, 2004). Changes in land cover and land use resulting from human activities, such as deforestation, forest logging, road construction, fire and cultivation on steep slopes can have an important impact on landslide activity (Cannon, 2000; Glade, 2003). Much work has been done to evaluate the effect of logging and deforestation on landslides (e.g. Furbish and Rice, 1983; Ziemer et al., 1991).

Vegetation effects on slope stability may be broadly classified as either hydrological or mechanical in nature. The mechanical factors consist of reinforcement of soil by roots, surcharge, wind-loading and surface protection (Greenway, 1987). The effects of vegetation cover on the hydrological processes of shallow landsliding can be subdivided into the loss of precipitation by interception, removal of soil moisture by evapotranspiration and the effects on hydraulic conductivity (Van Beek, 2002; Wilkinson et al., 2002a,b). Use of remote sensing data for quantifying the hydrological properties of vegetation for landslide hazard assessment is not widely explored, though such methods are capable of providing spatially and temporally continuous parameters for a distributed dynamic assessment of landslides (Sekhar et al., 2006). For a deterministic dynamic assessment it is very important to have temporal landuse/landcover maps and the respective changes manifested in the mechanical and hydrological effects of vegetation. It is observed that of all the vegetation effects, root reinforcement dominates in its contribution to stability. In order to be able to carry out a probabilistic analysis using different sets of landslide distribution from different periods, it is very important that land use maps from these same periods are available, or better land use change maps.

Land use maps are made on a routine basis from medium resolution satellite imagery such as LANDSAT, SPOT, ASTER, IRS1-D, etc. Although change detection techniques such as post-classification comparison, temporal image differencing, temporal image ratioing, or Bayesian probabilistic methods have been widely applied in land use applications, fairly limited work has been done on the inclusion of multi-temporal land use change maps in landslide hazard studies (Mantovani et al., 1996).

Landslide hazard and risk maps are generated for the future, and therefore the expected changes in land use should be taken into account in the analysis, through the modeling of different land use change scenarios. For the analysis of the transitional probabilities of expected changes in the near future Markov Chain analysis has proven to be a useful tool (e.g. Balzter, 2000).

4.6. Triggering factors

Information related to triggering factors generally has more temporal than spatial importance, except when dealing with large areas on a small mapping scale. This type of data is related to rainfall, temperature and earthquake records over sufficiently large time periods, and the assessment of magnitude–frequency relations. Rainfall and temperature data are measured in individual meteorological stations, and earthquake data is normally available as earthquake catalogs. The spatial variation over the study area can be represented by interpolating the point data, provided that enough measurement data is available. For example a map of the maximum expected rainfall in 24 h for different return periods can be generated as the input in dynamic slope stability modeling. In the case of earthquake triggered landslides a map of the peak ground acceleration (PGA) with a 10% exceedance probability in 50 years could be used as input in subsequent infinite slope modeling. Such PGA maps are available for most of the seismically affected regions through the Global Seismic Hazard Assessment Project (Giardini et al., 1999).

For larger areas, if no data is available from meteorological stations, general rainfall estimates from satellite imagery can be used, such as from Tropical Rainfall Measuring Mission (TRMM) Multi-satellite Precipitation Analysis (TMPA), which is used to issue landslide warnings based on a threshold value derived from earlier published intensity–duration–frequency relationships for different countries (Hong et al., 2007). Hong and Adler (2007) propose an early warning system for global landslide warnings, based on the TRMM rainfall estimations, combined with the near-real time ground shaking prediction system for earthquakes (Wald et al., 2003) and with generalized landslide susceptibility information, including altitude information from SRTM, and landcover information, derived from MODIS. The use of weather radar for rainfall prediction in landslide studies is a field which is very promising (e.g. Crosta and Frattini, 2003; Maki et al., 2005).

However, in order to be able to link these triggering factors with landslide dates, an extensive landslide inventory database is required in which the landslide are dated, either individually, or through the generation of event-based landslide inventory maps. Hong Kong is one of the few places in the world that has such extensive data collected over the past forty years which, linked to a network of over

Please cite this article as: van Westen, C.J., et al., Spatial data for landslide susceptibility, hazard, and vulnerability assessment: An overview, Engineering Geology (2008), doi:10.1016/j.enggeo.2008.03.010

65 weather stations, allows the generation of accurate relationships between rainfall duration/intensity and landslide density (Yu et al., 2007).

5. Elements at risk information

Elements at risk inventories can be carried out at various levels, depending on the requirement of the study. Table 6 gives a more detailed description of the main points.

Often the basic units for risk analysis could be derived from existing cadastral databases, and population data may be derived from existing census data. Even if digital information is available, a considerable amount of work needs to be done in developing a GIS database for elements at risk mapping, which will include the characterization of the building types, mapping of temporal building occupancies, and collection of population information through field inquiries. A common problem found is that there is no link between non-spatial data (e.g. housing data) and spatial data (e.g. building footprints). Also here the use of mobile GIS is essential (Montoya, 2003). If no digital data exist, the elements at risk can be digitized from high resolution images. Also intends have been made to automatically extract buildings from InSAR (Stilla et al., 2003), LiDAR (Priestnall et al., 2000) and IKONOS (Fraser et al., 2002).

Fig. 7 gives an illustration of the various levels of elements at risk data that were available for the city of Tegucigalpa. The basic information was available in the form of individual building footprints, which lacked any attribute information. This level was considered too detailed as data collection for each individual building was too expensive. On the other hand, most of the attribute information related to population was linked to a polygon map of the wards of the city ("colonias" in Spanish, see Fig. 7C). The detail of these units was considered too low, as landslide hazard varies significantly within one ward, and the integration of hazard data with general ward data would lead to non-reliable results. Therefore so-called mapping units were introduced as an intermediate level of elements at risk. They are considered to be more or less homogeneous units with respect to buildings types, socio-economic level and urban land use (See Fig. 7B). These mapping were generated through image interpretation using the very high resolution imagery, and their boundaries are mostly formed by streets. The attributes from the higher and the lower levels were then converted to this intermediate level. For instance, the number of buildings per mapping unit was measured by overlaying the building footprint map with the mapping unit map. The average height of the elements at risk was estimated using the difference between the LiDAR DEM and the surface DEM generated from the contourlines with 2.5 m contour interval, in the location of the building footprints (See Fig. 7D). Information of predominant urban land use was not available, and therefore had to be generated, based on detailed image interpretation (See Fig. 7E). Population information was only available at ward level (Fig. 7C), and the population values had to be distributed over the mapping units, based on the urban landuse, the height of the buildings and the footprint area, from which the total floor area per mapping unit and landuse class could be calculated. Population density was also calculated for different temporal scenarios (e.g. daytime/nighttime/commuting time) using the urban landuse as the main criteria. Fig. 7 illustrates the need for

Table 6
Main elements at risk used in landslide risk assessment studies, and how they can be spatially represented in the four defined mapping scales

Type of elements at risk	Scale of analysis			
	Small	Medium	Large	Detailed
Buildings	By Municipality •Nr. buildings	Mapping units •Predominant land use •Nr. Buildings	Building footprints •Generalized use •Height •Building types	Building footprints •Detailed use •Height •Building types •Construction type •Quality/age •Foundation
Transportation networks	General location of transportation networks	Road & railway networks, with general traffic density information	All transportation networks with detailed classification, including viaducts etc. & traffic data	All transportation networks with detailed engineering works & detailed dynamic traffic data
Lifelines	Main powerlines	Only main networks •Water supply •Electricity	Detailed networks: •Water supply •Waste water •Electricity •Communication •Gas	Detailed networks and related facilities: •Water supply •Waste water •Electricity •Communication •Gas
Essential facilities	By Municipality •Number of essential facilities	As points •General characterization •Buildings as groups	Individual building footprints •Normal characterization •Buildings as groups	Individual building footprints •Detailed characterization •Each building separately
Population data	By Municipality •Population density •Gender •Age	By ward •Population density •Gender •Age	By Mapping unit •Population density •Daytime/nighttime •Gender •Age	People per building •Daytime/nighttime •Gender •Age •Education
Agriculture data	By Municipality •Crop types •Yield information	By homogeneous unit, •Crop types •Yield information	By cadastral parcel •Crop types •Crop rotation •Yield information •Agricultural buildings	By cadastral parcel, for a given period of the year •Crop types •Crop rotation & time •Yield information
Economic data	By region •Economic production •Import/export •Type of economic activities	By Municipality •Economic production •Import/export •Type of economic activities	By Mapping unit •Employment rate •Socio-economic level •Main income types Plus larger scale data	By building •Employment •Income •Type of business Plus larger scale data
Ecological data	Natural protected areas with international approval	Natural protected area with national relevance	General flora and fauna data per cadastral parcel.	Detailed flora and fauna data per cadastral parcel

Please cite this article as: van Westen, C.J., et al., Spatial data for landslide susceptibility, hazard, and vulnerability assessment: An overview, Engineering Geology (2008), doi:10.1016/j.enggeo.2008.03.010

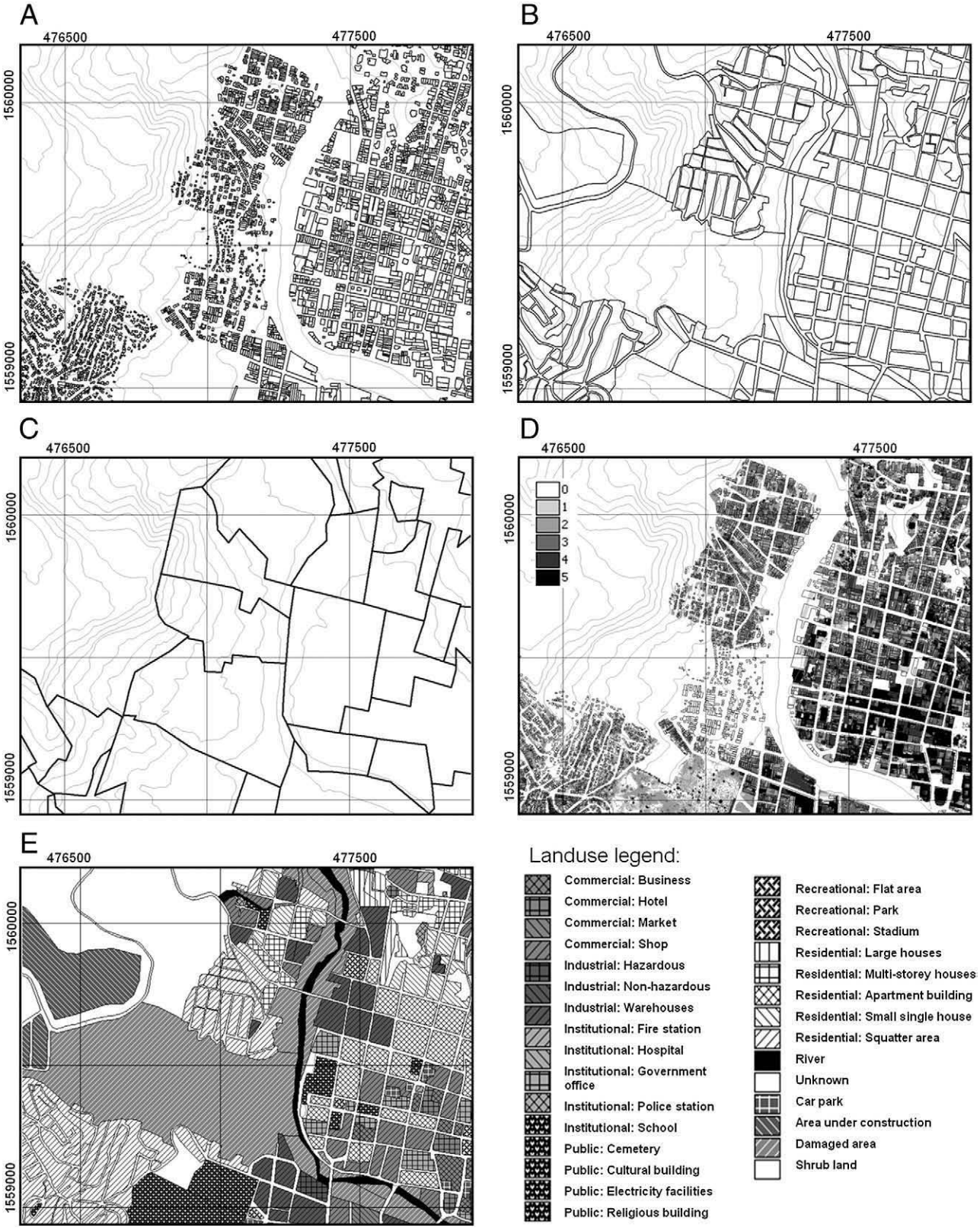

Fig. 7. Different types of information that are important for the generation of an elements at risk database in Tegucigalpa. A: Individual building footprints, B: Mapping units, representing zones of more or less homogeneous urban landuse and building types, C: Wards (locally called Colonies), D: Building height, in number of stories, E: Landuse classification of the mapping units.

regular updating of the element at risk database. The building footprint map (Fig. 7A) still contains the buildings of the Colonia Soto and nearby neighbourhoods that were destroyed by the El Berrinche landslide and flooding during Hurricane Mitch.

6. Conclusions

As can be seen from Table 1 landslide risk assessment can be carried out on different scales, using different methods for susceptibility and

Please cite this article as: van Westen, C.J., et al., Spatial data for landslide susceptibility, hazard, and vulnerability assessment: An overview, Engineering Geology (2008), doi:10.1016/j.enggeo.2008.03.010

hazard assessment and can be qualitative or quantitative in nature. The optimal selection of the scale and method are strongly depending on the availability of spatial information. Each type of analysis requires a number of crucial data layers, without which the analysis is not possible, apart from a whole range of other data.

There are several pitfalls in this process that should be avoided. Some of these are mentioned below:

- Selection of a method that does not suit the available data and the scale of the analysis. For instance, selecting a physical modeling approach at small scales with insufficient geotechnical and soil depth data. This will either lead to large simplifications in the resulting hazard and risk map, or to endless data collection. Another example of this is the selection of a statistical modeling approach in very homogenous areas, or in areas with very few landslides.
- Use of incomplete landslide inventories, either in temporal aspect, in the landslide classification, or in separating the erosional from the accumulational part. Although landslide inventories will never be complete, it is important to keep in mind that different landslide types are controlled by different combinations of environmental and triggering factors.
- Using the same type of data and method of analysis for entirely different landslide types and failure mechanisms. There are many examples from literature where all past landslide events have been used in a statistical analysis, leading to very general results. The inventory should be subdivided into several subsets, each related to a particular failure mechanism, and linked to a specific combination of causal factors. Also only those parts of the landslides should be used that represent the situation of the slopes that failed. This is illustrated for the Tegucigalpa area in Fig. 8, which contains four

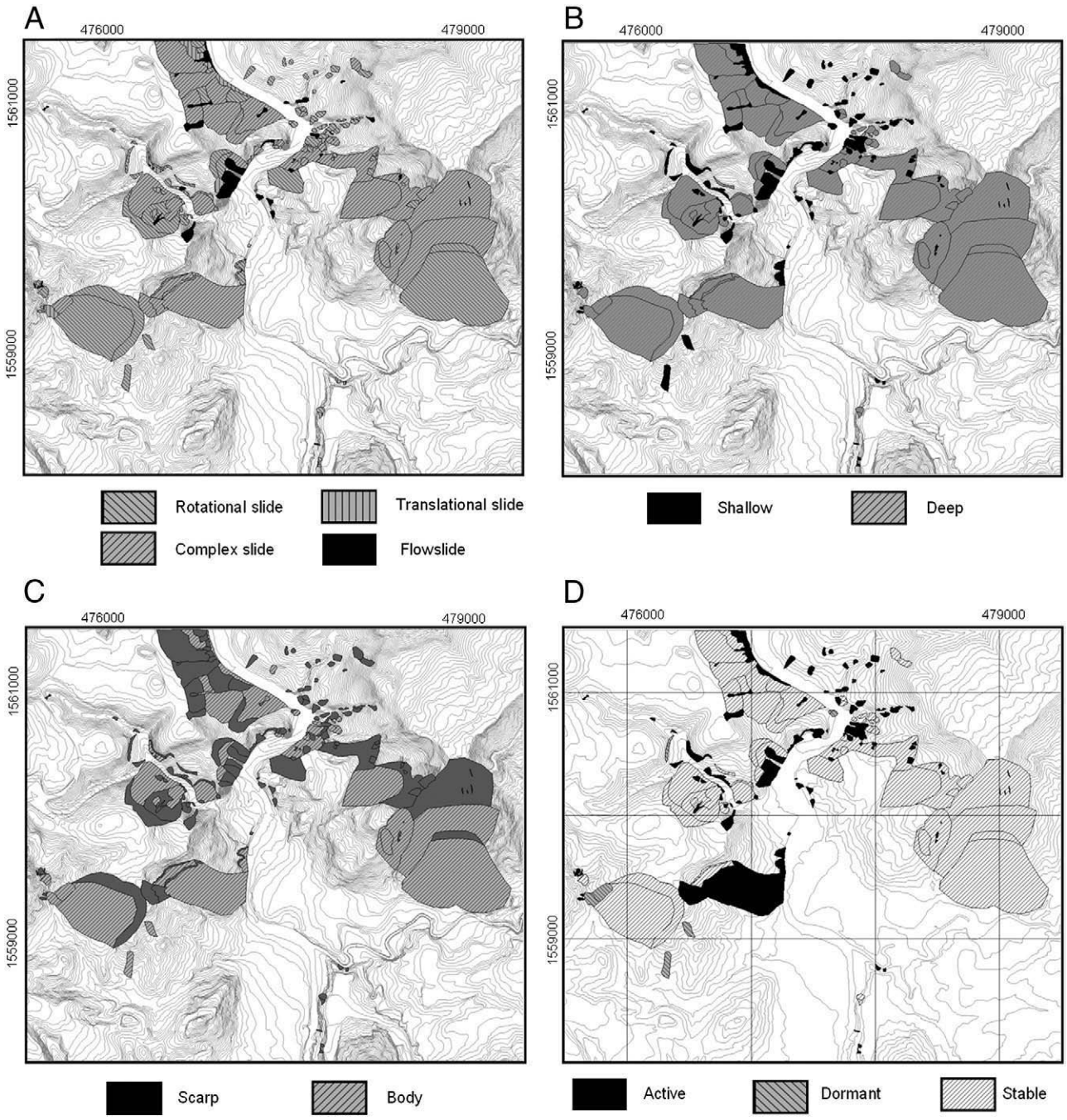

Fig. 8. Classification of landslides in Tegucigalpa. A: landslide types, B: landslide depth, C: landslide components, D: landslide activity.

Please cite this article as: van Westen, C.J., et al., Spatial data for landslide susceptibility, hazard, and vulnerability assessment: An overview, Engineering Geology (2008), doi:10.1016/j.enggeo.2008.03.010

different aspects of landslide classification, related to type, depth, components and activity that are relevant for the evaluation of the relationship with environmental and triggering factors.
- Use of data with a scale or detail that is not appropriate for the hazard assessment method selected. For instance, using an SRTM DEM to calculate slope angles used in statistical hazard assessment.
- Selection of easily obtainable landslide causal factors, such as DEM derivatives from SRTM data on a medium or large scale, or the use of satellite derived NDVI values as a causal factor instead of generating a land cover map.
- Use factor maps that are not from the period of the landslide occurrence. For instance, in order to be able to correlate landslides with landuse/landcover changes, it is relevant to map the situation that existed when the landslide occurred, and not the situation that resulted after the landslide.
- On the other hand also the use of outdated factor maps for predicting landslides should be avoided. Although relationships between factors and landslides should be established for the period in which the landslides were formed, it is important to use up to date maps that represent the actual situation for predicting events in the near future.

Much of the landslide susceptibility and hazard work is based on the assumption that "the past is key to the future", and that historical landslides and their causal relationships can be used to predict future ones. However, one could also follow the analogy of the investment market in stating that "results obtained in the past are not a guarantee for the future". Conditions under which landslide happened in the past change, and the susceptibility, hazard and risk maps are made for the present situation. As soon as there are changes in the causal factors (e.g. a road with steep cuts is constructed in a slope which was considered as low hazard before) or changes in the elements at risk (e.g. city growth) the hazard and risk information needs to be adapted.

The spatial data for landslide risk, as indicated in Table 1, is coming from many different sources and disciplines. The more data sources involved the more complicated the study as every organization has its own rules on data production. This is particularly relevant in developing countries where most information is still in analog format or where the digital information is produced without consistent and interoperable standards. However, also in developing countries a number of the crucial data sets as listed in Table 1 can now be obtained with the help of low cost satellite information, e.g. through the use of SRTM, ASTER and even Google Earth, as large parts of the world are now covered by very high resolution images. Nevertheless there is always a trade-off between the quality of the data and the cost/resources involved and the reliability of the hazard/risk assessment. In order to achieve the best quality/cost relation, it is very important to invest in landslide inventory databases. Landslide inventory databases are very important for generating reliable prediction maps of spatial and temporal probability for landslides. Multi-temporal landslide information is essential to new approaches for the generation of quantitative landslide probability maps (e.g., Coe et al., 2004; Chung and Fabbri, 2005 and Guzzetti et al., 2005). New developments in digital data collection have facilitated the collection of landslide information; especially the wider availability of high resolution satellite imagery with stereo capabilities that are finally a good substitute for aerial photographs. Emphasis should be given to the generation of event-based landslide inventory maps that are related to particular triggering events.

A relation between triggering events (rainfall or earthquakes) and landslide occurrences is needed in order to be able to assess the temporal probability. Temporal probability assessment of landslides is either done using rainfall threshold estimation, through the use of multi-temporal data sets in statistical modeling, or through dynamic modeling. Rainfall threshold estimation is mostly done using antecedent rainfall analysis, for which the availability of a sufficient number of landslide occurrence dates is essential. If distribution maps are available of landslides that have been generated during the same triggering event, a useful approach is to derive susceptibility maps using statistical or heuristic methods, and link the resulting classes to the temporal probability of the triggering events (e.g. Zezere et al., 2005). The most optimal method for estimating both temporal and spatial probability is dynamic modeling, where changes in hydrological conditions are modeled using daily (or larger) time steps based on rainfall data. However, more emphasis should be given to the collection of reliable input maps, focusing on soil types and soil thickness. The methods for hazard analysis should be carried out for different landslide types and volumes, as these are required for the estimated damage potential. Landslide hazard is both related to landslide initiation, as well as to landslide deposition, and therefore also landslide run out analysis should be included on a routine basis.

A good understanding and quantification of the different hazard aspects (temporal and spatial probability of initiation, magnitude–frequency relation and run out potential) is essential in order to be able to make further advancements in landslide vulnerability assessment (e.g. Guzzetti et al., 2005). Also more emphasis could be given to the collection of historic landslide damage information for different elements at risk, and relate these to the characteristics of the landslides that caused the damage (e.g. volume, speed, run-out length).

Eventually, it is the spatial data availability that is the limiting factor in landslide hazard and risk assessment.

Acknowledgements

The authors would like to thank Gonzalo Funes Siercke, Annemarie Ebert, and Norman Kerle, for their support in getting the data for Tegucigalpa. This research was supported by the United Nations University — ITC School on Disaster Geo-Information Management.

References

Ackermann, F., 1999. Airborne Laser Scanning — Present Status and Future Expectations. ISPRS Journal of Photogrammetry and Remote Sensing 54, 64–67.
Ardizzone, F., Cardinali, M., Carrara, A., Guzzetti, F., Reichenbach, P., 2002. Impact of mapping errors on the reliability of landslide hazard maps. Natural Hazards and Earth System Sciences 2, 3–14.
Asselen, S.V., Seijmonsbergen, A.C., 2006. Expert-driven semi-automated geomorphological mapping for a mountainous area using a laser DTM. Geomorphology 78 (3–4), 309–320.
Atkinson, P.M., Massari, R., 1998. Generalized linear modeling of susceptibility to landsliding in the central Appennines, Italy. Computers & Geosciences 24 (4), 373–385.
Balzter, H., 2000. Markov chain models for vegetation dynamics. Ecological Modelling 126, 139–154.
Barlow, J., Martin, Y., Franklin, S.E., 2003. Detecting translational landslide scars using segmentation of Landsat ETM+ and DEM data in the northern Cascade Mountains, British Columbia. Canadian Journal of Remote Sensing 29, 510–517.
Bianchi, R., Cavalli, R.M., Fiumi, L., Marino, C.M., Pignatti, S., 1999. Airborne MIVIS hyperspectral imaging spectrometer over natural and anthropic areas. Proceedings of the Fourth International Airborne Remote Sensing Conference and Exibition/21st Canadian Symposium on Remote Sensing, vol. 1. Ottawa, Ont., Canada, pp. 337–344.
Brabb, E.E., Pampeyan, E.H., Bonilla, M.G., 1978. Landslide susceptibility in San Mateo County, California. US Geological Survey Miscellaneous Field Studies Map, MF-360, Map at 1: 62,500 scale.
Cannon, S.H., 2000. Debris flow response of southern California watersheds burned by wildfire. In: Wieczorec, G.F., Naeser, N.D. (Eds.), Debris Flow Hazards Mitigation: Mechanics, Prediction and Assessment. A.A. Balkema Publishers, Rotterdam, pp. 45–52.
Cardinali, M., Reichenbach, P., Guzzetti, F., Ardizzone, F., Antonini, G., Galli., Cacciano, M., Castellani, M., Salvati, P., 2002. A geomorphological approach to the estimation of landslide hazards and risks in Umbria, Central Italy. Natural Hazards and Earth System Sciences 2, 57–72.
Carrara, A., Carratelli, E.P., Merenda, L., 1977. Computer-based data bank and statistical analysis of slope instability phenomena. Zeitschrift für Geomorphologie 21, 187–222.
Carrara, A., Cardinali, M., Guzzetti, F., Reichenbach, P., 1995. GIS-based techniques for mapping landslide hazard. In: Carrara, A., Guzzetti, F. (Eds.), Geographical Information Systems in Assessing Natural Hazards. Kluwer Academic Publications, Dordrecht, The Netherlands, pp. 135–176.
Carrara, A., Guzzetti, F., Cardinali, M., Reichenbach, P., 1999. Use of GIS technology in the prediction and monitorino of landslide hazard. Natural Hazards 20, 117–135.
Casadei, M., Dietrich, W.E., Miller, N.L., 2003. Testing a model for predicting the timing and location of shallow landslide initiation in soil-mantled landscapes. Earth Surface Processes and Landforms 28, 925–950.

Please cite this article as: van Westen, C.J., et al., Spatial data for landslide susceptibility, hazard, and vulnerability assessment: An overview, Engineering Geology (2008), doi:10.1016/j.enggeo.2008.03.010

Castellanos, E., Van Westen, C.J., 2008. Qualitative landslide susceptibility assessment by multicriteria analysis; a case study from San Antonio del Sur, Guant'anamo, Cuba. Geomorphology 94 (3–4), 453–466.
Catani, F., Farina, P., Moretti, S., Nico, G., Strozzi, T., 2005. On the application of SAR interferometry to geomorphological studies: estimation of landform attributes and mass movements. Geomorphology 66 (1–4), 119–131.
CEDD, 2007. The Natural Terrain Landslide Inventory. Civil Engineering and Development Department, Hong Kong. URL: http://hkss.cedd.gov.hk/hkss/eng/whatsnew/index.htm, Accessed on 30th June 2007.
Chau, K.T., Sze, Y.L., Fung, M.K., Wong, W.Y., Fong, E.L., Chan, L.C.P., 2004. Landslide hazard analysis for Hong Kong using landslide inventory and GIS. Computers & Geosciences 30 (4), 429–443.
Cheng, K.S., Wei, C., Chang, S.C., 2004. Locating landslides using multi-temporal satellite images. Advances in Space Research 33 (3), 296–301.
Chung, C.J., Fabbri, A., 2005. Systematic procedures of landslide hazard mapping for risk assessment using spatial prediction models. In: Glade, T., Anderson, M., Crozier, M.J. (Eds.), Landslide hazard and risk. John Wiley and Sons Ltd., West Sussex, England, pp. 139–174.
Claessens, L., Heuvelink, G.B.M., Schoorl, J.M., Veldkamp, A., 2005. DEM resolution effects on shallow landslide hazard and soil redistribution modeling. Earth Surface Processes and Landforms 30, 461–477.
CNR-IRPI, 2006. Sistema Informativo sulle Catastrofi Idrogeologiche (SICI). Gruppo Nazionale per la Difesa dalla Catastrofi Idrogeologiche (GNDCI). del Consiglio Nazionale delle ricerche (CNR). URL: http://sicimaps.irpi.cnr.it/website/sici/viewer.htm. Accessed on 30th June 2007.
Coe, J.A., Michael, J.A., Crovelli, R.A., Savage, W.Z., 2004. Probabilistic assessment of precipitation-triggered landslides using historical records of landslide occurrence, Seattle, Washington. Environmental Engineering Geosciences 10, 103–122.
Corominas, J., Baeza, C., Saluela, I., 1992. The influence of geometrical slope characteristics and land use on the development of shallow landslides. In: Bell, D.H. (Eds.), Proceedings of the 6th International Symposium on Landslides, 10–14 February, Christchurch, New Zealand. A.A. Balkema Publishers, Rotterdam, The Netherlands, pp. 919–924.
Crosta, G.B., Frattini, P., 2003. Distributed modelling of shallow landslides triggered by intense rainfall. Natural Hazards and Earth System Sciences 3 (1–2), 81–93.
Cruden, D.M., Varnes, D.J., 1996. Landslide types and processes. In: Turner, A.K., Schuster, R.L. (Eds.), Landslides, Investigation and Mitigation. Transportation Research Board, Special Report 247, Washington D.C., USA, pp. 36–75.
De Graaff, L.W.S., De Jong, M.G.G., Rupke, J., Verhofstad, J., 1987. A geomorphological mapping system at scale 1:10,000 for mountainous areas. Zeitschrift für Geomorphologie 13, 229–242.
Dewitte, O., Demoulin, A., 2005. Morphometry and kinematics of landslides inferred from precise DTMs in West Belgium. Natural Hazards and Earth System Sciences 5 (2), 259–265.
Dietrich, W.E., Montgomery, D.R., 1998. Shalstab: a digital terrain model for mapping shallow landslide potential. URL: http://socrates.berkeley.edu/~geomorph/shalstab/. Accessed on 30th June 2007.
Dietrich, W.E., Reiss, R., Hsu, M., Montgomery, D.R., 1995. A process-based model for colluvial soil depth and shallow landsliding using digital elevation data. Hydrological Processes 9, 383–400.
Farr, T.G., et al., 2007. The shuttle radar topography mission. Review of Geophysics 45 RG2004. doi:10.1029/2005RG000183.
Ferretti, A., Prati, C., Rocca, F., 2001. Permanent scatterers in SAR interferometry. IEEE Transactions on Geoscience and Remote Sensing 39 (1), 8–20.
Fraser, C.S., Baltsavias, E., Gruñe, A., 2002. Processing of IKONOS imagery for submetre 3D positioning and building extraction. ISPRS Journal of Photogrammetry and Remote Sensing 56 (3), 177–194.
Fujisada, H., Bailey, G.B., Kelly, G.G., Hara, S., Abrams, M.J., 2005. ASTER DEM performance. IEEE Transactions on Geoscience and Remote Sensing 43 (12), 2707–2714.
Furbish, D.J., Rice, R.M., 1983. Predicting landslides related to clearcut logging, Northwestern California, USA. Mountain Research and Development 3, 253–259.
Geoscience Australia, 2006. Australian Landslides Database. Australian Government, Geoscience Australia. http://www.ga.gov.au/oracle/landslid/landsl_online.jsp. Accessed on 30th June 2007.
Giardini, D., Grunthal, G., Shedlock, K.M., 1999. The GSHAP Global Seismic Hazard Map. Annali di Geofisica 42 (6), 1225–1230.
Giles, P.T., Franklin, S.E., 1998. An automated approach to the classification of the slope units using digital data. Geomorphology 21, 251–264.
Glade, T., 2001. Landslide hazard assessment and historical landslide data — an inseparable couple? In: Glade, T., Albini, P., Frances, F. (Eds.), The Use of Historical Data in Natural Hazards Assessment (Advances in Natural and Technological Hazard Research). Kluwer Academic Publications, Dordrecht, The Netherlands, pp. 153–168.
Glade, T., 2003. Landslide occurrence as a response to land use change: a review of evidence from New Zealand. CATENA 51 (3–4), 297–314.
Glade, T., Crozier, M.J., 1996. Towards a national landslide information base for New Zealand. New Zealand Geographer 52 (1), 29–40.
Glade, T., Crozier, M.J., 2005. A review of scale dependency in landslide hazard and risk analysis. In: Glade, T., Anderson, M., Crozier, M.J. (Eds.), Landslide Hazard and Risk. John Wiley and Sons Ltd, West Sussex, England, pp. 75–138.
Glenn, N.F., Streutker, D.R., Chadwick, D.J., Thackray, G.D., Dorsch, S.J., 2006. Analysis of LiDAR-derived topographic information for characterizing and differentiating landslide morphology and activity. Geomorphology 73, 131–148.
Greenway, D.R., 1987. Chapter 6: vegetation and slope stability. In: Anderson, M.G., Richards, K.S. (Eds.), Slope Stability. John Wiley and Sons Ltd., West Sussex, England.
Grignon, A., Bobrowsky, P., Coultish, T., 2004. Landslide database management philosophy in the Geological Survey of Canada. Geo-Engineering for the Society and its Environment. Proceedings of the 57th Canadian Geotechnical Conference and the 15th joint CGS-IAAH Conference, 24–27 October, Québec, Canada. A.A. Balkema Publishers, Rotterdam, The Netherlands.
Gustavsson, M., Kolstrup, E., Seijmonsbergen, A.C., 2006. A new symbol and GIS based detailed geomorphological mapping system: renewal of a scientific discipline for understanding landscape development. Geomorphology 77, 90–111.
Gutierrez, R., Gibeaut, J.C., Smyth, R.C., Hepner, T.L., Andrews, J.R., 2001. Precise airborne LiDAR surveying for coastal research and geohazards applications. International Archives on Photogrammetry and Remote Sensing, Volume XXXIV-3/W4, Annapolis, MD, 22–24 Oct. 2001, pp. 185–192.
Guzzetti, F., 2000. Landslide fatalities and the evaluation of landslide risk in Italy. Engineering Geology 58 (2), 89–107.
Guzzetti, F., Tonelli, G., 2004. Information system on hydrological and geomorphological catastrophes in Italy (SICI): a tool for managing landslide and flood hazards. Natural Hazards and Earth System Sciences 4, 213–232.
Guzzetti, F., Cardinali, M., Reichenbach, P., 1994. The AVI project: a bibliographical and archive inventory of landslides and floods in Italy. Environmental Management 18 (4), 623–633.
Guzzetti, F., Reichenbach, P., Cardinali, M., Galli, M., Ardizzone, F., 2005. Probabilistic landslide hazard assessment at the basin scale. Geomorphology 72, 272–299.
Haneberg, W.C., 2004. The ins and outs of airborne LiDAR: an introduction for practicing engineering geologists. AEG News 48 (1), 16–19.
Harp, E.L., Castañeda, M.R., Held, M.D., 2002a. Landslides triggered by Hurricane Mitch in Tegucigalpa, Honduras. U.S. Geological Survey Open-File Report 02-33. 11 pp., 1 plate.
Harp, Edwin L., Held, Matthew D., Castañeda, Mario, McKenna, Jonathan, P., Jibson, Randall, W., 2002b. Landslide hazard map of Tegucigalpa, Honduras. U.S. Geological Survey Open-File Report 02-219. 9 pp., 2 plates.
Hastings, D.A., Dunbar, P.K., 1998. Development and assessment of the global land 1 km base elevation digital elevation model (GLOBE). International Archives of Photogrammetry and Remote Sensing 32, 218–221 Part 4.
Haugerud, R.A., Harding, D.J., Johnson, S.Y., Harless, J.L., Weaver, C.S., Sherrod, B.L., 2003. High-resolution LiDAR topography of the Puget Lowland, Washington — a bonanza for earth science. GSA Today 13, 4–10.
Henry, J.B., Malet, J.P., Maquaire, O., Grussenmeyer, P., 2002. The use of small-format and low-altitude aerial photos for the realization of high-resolution DEMs in mountainous areas: application to the Super-Sauze earthflow (Alpes-de-Haute-Provence, France). Earth Surface Processes and Landforms 27, 1339–1350.
Hervas, J., Barredo, J.I., Rosin, P.L., Pasuto, A., Mantovani, F., Silvano, S., 2003. Monitoring landslides from optical remotely sensed imagery: the case history of Tessina landslide, Italy. Geomorphology 54, 63–75.
Hirano, A., Welch, R., Lang, H., 2003. Mapping from ASTER stereo image data: DEM validation and accuracy assessment. ISPRS Journal of Photogrammetry & Remote Sensing 57, 356–370.
Hong, Y., Adler, R.F., 2007. Towards an early-warning system for global landslides triggered by rainfall and earthquake. International Journal of Remote Sensing 28 (16), 3713–3719.
Hong, Y., Adler, R.F., Negri, A., Huffman, G.J., 2007. Flood and landslide applications of near real-time satellite rainfall estimation. Natural Hazards 43 (2), 285–294.
Hsiao, K.H., Liu, J.K., Yu, M.F., Tseng, Y.H., 2004. Change detection of landslide terrains using ground-based LiDAR data. XXth ISPRS Congress, Istanbul, Turkey, Commission VII, WG VII/5. 5 pp.
IAEG-Commission on Landslides, 1990. Suggested nomenclature for landslides. Bulletin of the International Association of Engineering Geology 41, 13–16.
Ibsen, M., Brunsden, D., 1996. The nature, use and problems of historical archives for the temporal occurrence of landslides, with specific reference to the south coast of Britain, Ventnor, Isle of Wight. Geomorphology 15, 241–258.
IGOS, 2003. In: Marsh, S., Paganini, M., Missotten, R. (Eds.), Geohazards Team Report. http://igosg.brgm.fr/. Accessed on 30th June 2007.
INETER, 2006. Inventario nacional de deslizamientos en Nicaragua. Instituto Nicaragüense De Estudios Territoriales. URL: http://mapserver.ineter.gob.ni/website/Mapas/desli/viewer.htm. Accessed on 30th June 2007.
IUGS—Working group on landslide, 1995. A suggested method for describing the rate of movement of a landslide. Bulletin of the International Association of Engineering Geology 52, 75–78.
IUGS-Working group on landslide, 2001. A suggested method for reporting landslide remedial measures. Bulletin of Engineering Geology and Environment 60, 69–74.
JICA, 2002. The study on flood control and landslide prevention in the Tegucigalpa metropolitan area of the Republic of Honduras. Japan International Cooperation Agency Interim Report. 148 pp.
Jones, L.D., 2006. Monitoring landslides in hazardous terrain using terrestrial LiDAR: an example from Montserrat. The Quarterly Journal of Engineering Geology and Hydrogeology 39 (4), 371–373.
JTC-1 Joint Technical Committee on Landslides and Engineered Slopes, 2008. Guidelines for landslide susceptibility, hazard and risk zoning, for land use planning. Engineering Geology (this volume).
Klimaszewski, M., 1982. Detailed geomorphological maps. ITC Journal 3, 265–271.
Kramer, J.H., 2000. Digital Mapping Techniques '00-Workshop Proceedings. U.S. Geological Survey Open-File Report 00-325. URL: http://pubs.usgs.gov/of/of00-325/. Accessed on 30th June 2007.
Lang, A., Moya, J., Corominas, J., Schrott, L., Dikau, R., 1999. Classic and new dating methods for assessing the temporal occurrence of mass movements. Geomorphology 30 (1–2), 33–52.
Lee, S., Chwae, U., Min, K., 2002. Landslide susceptibility mapping by correlation between topography and geological structure: the Janghung area, Korea. Geomorphology 46 (3–4), 149–162.
Maki, M., Iwanami, K., Misumi, R., Park, S.-G., Moriwaki, H., Maruyama, K., Watabe, I., Lee, D.-I., Jang, M., Kim, M.-K., Bringi, V.N., Uyeda, H., 2005. Semi-operational

Please cite this article as: van Westen, C.J., et al., Spatial data for landslide susceptibility, hazard, and vulnerability assessment: An overview, Engineering Geology (2008), doi:10.1016/j.enggeo.2008.03.010

rainfall observations with X-band multi-parameter radar. Atmospheric Science Letters 6, 12–18.
Mantovani, F., Soeters, R., Van Westen, C.J., 1996. Remote sensing techniques for landslide studies and hazard zonation in Europe. Geomorphology 15 (3–4), 213–225.
Martin, Y.E., Franklin, S.E., 2005. Classification of soil- and bedrock-dominated landslides in British Columbia using segmentation of satellite imagery and DEM data. International Journal of Remote Sensing 26, 1505–1509.
Mastin, M.C., 2002. Flood-hazard mapping in Honduras in response to Hurricane Mitch. U.S. Geological Survey Water-Resources Investigations Report 01-4277. 46 pp.
McKean, J., Roering, J., 2004. Objective landslide detection and surface morphology mapping using high-resolution airborne laser altimetry. Geomorphology 57, 331–351.
Metternicht, G., Hurni, L., Gogu, R., 2005. Remote sensing of landslides: an analysis of the potential contribution to geo-spatial systems for hazard assessment in mountainous environments. Remote Sensing of Environment 98 (23), 284–303.
Miliaresis, G.C., 2001. Geomorphometric mapping of Zagros Ranges at regional scale. Computers & Geosciences 27, 775–786.
Montoya, L., 2003. Geo-data acquisition through mobile GIS and digital video: an urban disaster management perspective. Environmental Modelling & Software 18 (10), 869–876.
Moore, I.D., Grayson, R.B., Ladson, A.R., 2001. Digital terrain modelling: a review of hydrological, geomorphological, and biological applications. Hydrological Processes 5 (1), 3–30.
NGU, 2006. National landslide database. Norwegian Geological Survey, Trondheim Norway. URL: http://www.skrednett.no/. Accessed on 30th June 2007.
Nichol, J., Wong, M.S., 2005. Satellite remote sensing for detailed landslide inventories using change detection and image fusion. International Journal of Remote Sensing 26 (9), 1913–1926.
NIED, 2006. Landslide Map Database. National Research Institute for Earth Science and Disaster Prevention, and Japan Science and Technology Agency. URL: http://lsweb1.ess.bosai.go.jp/jisuberi/jisuberi_mini_Eng/main.asp. Accessed on 30th June 2007.
Oka, N., 1998. Application of photogrammetry to the field observation of failed slopes. Engineering Geology 50 (1–2), 85–100.
Olsen, R.S., Villanueva, E., 2007. Geotechnical evaluation of the massive El Berrinche landslide in Honduras. In: Schaefer, V.L., Schuster, R.L., Turner, A.K. (Eds.), Proceedings of the First North American Landslide Conference, June 2007, Vail, Colorado, USA, pp. 738–748.
Peñalba, R.F., Kung, G.T.C., Juang, C.H., 2007. El Berrinche landslide in Honduras. In: Schaefer, V.L., Schuster, R.L., Turner, A.K. (Eds.), Proceedings of the First North American Landslide Conference, June 2007, Vail, Colorado, USA, pp. 730–737.
Pike, R.J., 2000. Geomorphometry — diversity in quantitative surface analysis. Progress in Physical Geography 24 (1), 1–20.
Priestnall, G., Jaafar, J., Duncan, A., 2000. Extracting urban features from LiDAR digital surface models. Computers, Environment and Urban Systems 24 (2), 65–78.
Rabus, B., Eineder, M., Roth, A., Bamler, R., 2003. The shuttle radar topography mission — a new class of digital elevation models acquired by spaceborne radar. ISPRS Journal of Photogrammetry and Remote Sensing 57 (4), 241–262.
Reid, L.M., Page, M.J., 2002. Magnitude and frequency of landsliding in a large New Zealand catchment. Geomorphology 49, 71–88.
Reidel, B., Walther, A., 2008. InSAR processing for the recognition of landslides. Advances in Geociences 14, 189–194.
Restrepo, C., Alvarez, N., 2006. Landslides and their contribution to land-cover change in the mountains of Mexico and Central America. Biotropica 38 (4), 446–457.
Roessner, S., Wetzel, H.U., Kaufmann, H., Sarnagoev, A., 2005. Potential of satellite remote sensing and GIS for landslide hazard assessment in southern Kyrgyzstan (Central Asia). Natural Hazards 35, 395–416.
Rogers, R.D., O'Conner, y E.A., 1993. Mapa Geológico de Honduras: Hoja de Tegucigalpa (segunda edicion), Instituto Geográfico Nacional, Tegucigalpa, Honduras, escala 1:50,000.
Rowbotham, D.N., Dudycha, D., 1998. GIS modelling of slope stability in Phewa Ta watershed, Nepal. Geomorphology 26 (1–3), 151–170.
Rowlands, K., Jones, L., Whitworth, M., 2003. Landslide laser scanning: a new look at an old problem. Quarterly Journal of Engineering Geology and Hydrogeology 36, 155–157.
Salciarini, D., Godt, J.W., Savane, W.Z., Conversini, P., Baum, R.L., Michael, J.A., 2006. Modeling regional initiation of rainfall-induced shallow landslides in the eastern Umbria Region of central Italy. Landslides 3, 181–194.
Schulz, W.H., 2004. Landslides mapped using LiDAR imagery, Seattle, Washington. U.S. Geological Survey Open-File Report 2004-1396.
Sekhar, L.K., et al., 2006. Effect of vegetation on debris flow initiation — conceptualisation and parameterisation of a dynamic model for debris flow initiation in Tikovil River Basin, Kerala, India, using PCRaster®. Proceedings of the 2nd International Symposium on Geo-information for Disaster Management, 25–26 September, Goa, India, Commission IV. International Society for Photogrammetry and Remote Sensing, Ahmadabad, India.
Singhroy, V., 2005. Remote sensing of landslides. In: Glade, T., Anderson, M., Crozier, M.J. (Eds.), Landslide Hazard and Risk. John Wiley and Sons Ltd., West Sussex, England, pp. 469–492.
Soeters, R., Van Westen, C.J., 1996. Slope instability recognition, analysis and zonation. In: Turner, A.K., Schuster, R.L. (Eds.), Landslides, investigation and mitigation. Transportation Research Board, National Research Council, Special Report 247. National Academy Press, Washington D.C., U.S.A., pp. 129–177.
Stilla, U., Soergel, U., Thoennessen, U., 2003. Potential and limits of InSAR data for building reconstruction in built-up areas. ISPRS Journal of Photogrammetry and Remote Sensing 58 (1–2), 113–123.
Terlien, M.T.J., Asch, T.W.J., Van Westen, C.J., 1995. Deterministic modelling in GIS-based landslide hazard assessment. In: Carrara, A., Guzzetti, F. (Eds.), Geographical Information System in Assessing Natural Hazard. Kluwer Academic Publications, New York, USA, pp. 57–77.
Tribe, S., Leir, M., 2004. The role of aerial photograph interpretation in natural hazard and risk assessment. Proceedings of the International Pipeline Conference, October 4–8, Calgary, Canada. 6 pp.
UNESCO-WP/WLI, 1993a. Multilingual Landslide Glossary. Bitech Publishers Ltd., Richmond, Canada. 34 pp.
UNESCO-WP/WLI, 1993b. A suggested method for describing the activity of a landslide. Bulletin of the International Association of Engineering Geology 47, 53–57.
UNESCO-WP/WLI, 1994. A suggested method for reporting landslide causes. Bulletin of the International Association of Engineering Geology 50, 71–74.
Van Beek, R., 2002. Assessment of the influence of changes in climate and land use on landslide activity in a Mediterranean environment. Netherlands Geographical Studies no 294, KNAG, Faculty of Geosciences, University of Utrecht. 366 pp.
Van Beek, L.P.H., Van Asch, T.W.J., 2004. Regional assessment of the effects of land-use change and landslide hazard by means of physically based modeling. Natural Hazards 30 (3), 289–304.
Van Westen, C.J., 2004. Geo-information tools for landslide risk assessment — an overview of recent developments. In: Lacerda, W., Ehrlich, M., Fontoura, S., Sayao, A. (Eds.), Landslides, Evaluation & Stabilization. Proceedings of the 9th International Symposium on Landslides, Rio de Janeiro, 28th June–2nd July, pp. 39–56.
Van Westen, C.J., Getahun, F.L., 2003. Analyzing the evolution of the Tessina landslide using aerial photographs and digital elevation models. Geomorphology 54 (1–2), 77–89.
Van Westen, C.J., Van Asch, T.W.J., Soeters, R., 2005. Landslide hazard and risk zonation; why is it still so difficult? Bulletin of Engineering geology and the Environment 65 (2), 167–184.
Wald, D., Wald, L., Worden, B., Goltz, J., 2003. ShakeMap — a tool for earthquake response. U.S. Geological Survey Fact Sheet 087-03.
Whitworth, M.C.Z., Giles, D.P., Murphy, W., 2005. Airborne remote sensing for landslide hazard assessment: a case study on the Jurassic escarpment slopes of Worcestershire, UK. Quarterly Journal of Engineering Geology and Hydrogeology 38 (3), 285–300.
Wilkinson, P.L., Anderson, M.G., Lloyd, D.M., Renaud, J.-P., 2002a. Landslide hazard and bioengineering: towards providing improved decision support through integrated numerical model development. Environmental Modelling & Software 17 (4), 333–344.
Wilkinson, P.L., Anderson, M.G., Lloyd, D.M., 2002b. An integrated hydrological model for rain-induced landslide prediction. Earth Surface Processes and Landforms 27, 1285–1297.
Wilson, J.P., Gallant, J.C., 2000. Digital terrain analysis. In: Wilson, J.P., Gallant, J.C. (Eds.), Terrain Analysis: Principles and Applications. John Wiley & Sons Ltd., New York, USA, pp. 1–27.
Xie, M., Tetsuro, E., Zhou, G., Mitani, Y., 2003. Geographic Information Systems based three-dimensional critical slope stability analysis and landslide hazard assessment. Journal of Geotechnical and Geoenvironmental Engineering 129 (12), 1109–1118.
Yu, Y.F., Lam, J.S., Siu, S.K., Pun, W.K., 2007. Recent advance in landslip warning system. In: Chan, R.K.S., et al. (Eds.), Thirty years of slope safety practice in Hong Kong. Special publication. Geotechnical Engineering Office, Civil Engineering and Development Department, Government of Hong Kong, pp. 298–303.
Zezere, J.L., Trigo, R.M., Trigo, I.F., 2005. Shallow and deep landslides induced by rainfall in the Lisbon region (Portugal): assessment of relationships with the North Atlantic Oscillation. Natural Hazards and Earth System Sciences 5, 331–344.
Zhou, Q., Liu, X., 2004. Analysis of errors of derived slope and aspect related to DEM data properties. Computers & Geosciences 30 (4), 369–378.
Ziemer, R.R., Lewis, J., Rice, R.M., Lisle, T.E., 1991. Modeling the cumulative effects of forest management strategies. Journal of Environmental Quality 20 (1), 36–42.

Please cite this article as: van Westen, C.J., et al., Spatial data for landslide susceptibility, hazard, and vulnerability assessment: An overview, Engineering Geology (2008), doi:10.1016/j.enggeo.2008.03.010